Arab American University

Faculty of Graduate Studies

Department of Health Sciences

Master Program in Molecular and Cellular Biosciences

Cell-Free Incorporation of Unnatural Photo-Cross Linkable Amino Acid p-Benzoyl-L-Phenylalanine (pBpa) Into γ-Secretase Subunit (Presenilin-1 (PS1))

Heba Shawkat Aref Kmail

202020404

Supervision Committee:

Prof. Hilal Zaid

Prof. Jörg Labahn

Dr. Siba Ismael

Dr. Ramzi Shawahna

This Thesis Was Submitted in Partial Fulfillment of the Requirements for the Master Degree in Molecular and Cellular Biosciences

Palestine, 2/2025

Arab American University

Faculty of Graduate Studies

Department of Health Sciences

Master Program in Molecular and Cellular Biosciences

Thesis Approval

Cell-Free Incorporation of Unnatural Photo-Cross Linkable Amino Acid p-Benzoyl-L-Phenylalanine (pBpa) Into γ-Secretase Subunit (Presenilin-1 (PS1))

Heba Shawkat Aref Kmail

202020404

This thesis was defended successfully on 5.2.2025 and approved by:

Thesis Committee Members:

Name	Title	Signature
1. Prof. Hilal Zaid	Main Supervisor	
2. Prof. Jörg Labahn	Co-Supervisor	
3. Dr. Siba Ismael	Member of Supervision Committee	
4. Dr. Ramzi Shawahna	Member of Supervision Committee	

Palestine, 2/2025

Declaration

I declare that, expect where explicit reference is made to the contribution of others, this thesis is substantially my own work and has not been submitted for any other degree at the Arab American University or any other institution.

Student Name: Heba Shawkat Aref Kmail

Student ID: 202020404

Signature: Heba Kmail

Date of Submitting the Final Version of the Thesis: 15.5.2025

Dedication

To my beloved family:

You are always the reason.

To Asmaa:

We did it!

To my professors, friends, and loved ones:

Your support and encouragement have made this journey unforgettable.

Heba Shawkat Aref Kmail

Acknowledgements

I am deeply grateful to the Centre for Structural Systems Biology (CSSB), Hamburg, Germany, for its inspiring and collaborative research environment. The resources, facilities, and expertise at CSSB have been instrumental to this research success. I also thank the Palestinian-German Science Bridge (PGSB) for their generous support in fostering scientific collaboration, providing essential resources, and enabling this international project.

My heartfelt gratitude goes to my home university, the Arab American University, for its academic foundation and support throughout my studies.

Special thanks to the technical and administrative staff at both CSSB and Arab American University for their invaluable assistance.

I would like to extend my sincere thanks to my supervisors, Prof. Hilal Zaid and Prof. Jörg Labahn, for their thoughtful guidance, insightful feedback, and unwavering support, which have been pivotal to my academic development.

I am particularly indebted to Dr. Siba Shanak for her belief in my abilities, mentorship, and constant inspiration.

I am grateful to Dr. Yajing Xiao for her collaboration, support, and shared knowledge.

I also deeply appreciate my research team—Tao, Guo, Aziz, Nishka, Devi, Jeney, and Lasha—for their enthusiasm, expertise, and dedication, which enriched my research journey. To my colleagues, faculty members, and lecturers, thank you for your insightful discussions, guidance, and encouragement that have significantly shaped my academic growth.

Heartfelt thanks to my friend and travel companion (Asmaa) for the beautiful laughs, the wonderful days, and for overcoming challenges together throughout my journey.

I owe my deepest thanks to my family, your belief in me has been my greatest strength and a source of constant motivation.

Thanks for my friends for their unwavering love, support, and patience throughout this journey.

Cell-Free Incorporation of Unnatural Photo-Cross Linkable Amino Acid p-Benzoyl-L-Phenylalanine (pBpa) Into γ-Secretase Subunit (Presenilin-1 (PS1))

Student Name: Heba Shawkat Aref Kmail

Prof. Hilal Zaid

Prof. Jörg Labahn

Dr. Siba Ismael

Dr. Ramzi Shawahna

Abstract

The γ-secretase (GS) complex is critical for regulating the processing of amyloid precursor protein (APP), which is intricately associated with the development of Alzheimer's disease (AD). The presenilin-1 (PS1) subunit, central of GS, contains the catalytic core necessary GS's proteolytic activity. Understanding PS1's structural and functional dynamics within the GS is crucial for elucidating PS1's role in AD.

Recent developments in protein engineering, especially the site-specific incorporation of unnatural amino acids (UAAs) like p-Benzoyl-L-phenylalanine (pBpa) through genetic code expansion, have improved the capacity to examine these dynamics. pBpa, can form covalent bonds with nearby residues when activated by ultraviolet (UV) light making it essential for investigating protein interactions and conformational changes.

This study aims to develop a Cell-Free Protein Synthesis (CFPS) system to incorporate the pBpa at the 190th amino acid position in PS1 using an amber stop codon and an orthogonal aminoacyl-tRNA synthetase (aaRS)/tRNA pair within an E. coli lysate-based CFPS system. This includes designing and optimizing of DNA templates, preparing of the required components, and refining of the CFPS system for efficient protein labeling and expression.

Methanococcus jannaschii tyrosyl-tRNA ($tRNA_{CUA}^{opt}$) was produced in BL21 Star™ (DE3) and isolated using the phenol-chloroform extraction method. Modified *Methanococcus jannaschii* tyrosyl-tRNA synthetase (Bpa-RS) was expressed in BL21γ::DE3 and purified using immobilized metal affinity chromatography (IMAC). The CFPS system was optimized using enhanced green fluorescent protein (eGFP) as a reporter. Agarose gel electrophoresis, sodium dodecyl-sulfate polyacrylamide gel electrophoresis (SDS-PAGE) and western blot were used for analysis.

Key plasmids and proteins for CFPS system were successfully verified. Double digestion and electrophoresis verified the existence of the Bpa-RS, $tRNA_{CUA}^{opt}$, PS1-N190-amber, and GFP genes. Bpa-RS and TEV protease were successfully expressed and purified with the correct size bands verified by SDS-PAGE and western blot. The optimal volume ratio of Bpa-RS to TEV protease was established for effective His-tag cleavage. tRNA was effectively expressed

and isolated. The truncated PS1 version resulted from the CFPS system, indicating a need for further optimization to incorporate pBpa efficiently.

Key aspects of the CFPS system for PS1 protein synthesis, including plasmid verification, expression and purification of Bpa-RS, tRNA isolation, and plasmid amount optimization, were successfully addressed in this study. However, further optimization is required in order to yield full-length PS1. The outcomes underscore CFPS's potential in protein synthesis and its applications in drug discovery, industrial biotechnology, and synthetic biology, especially in developing treatments for diseases like AD.

This study was conducted in the laboratories of the Centre for Structural Systems Biology (CSSB) in Hamburg, Germany, from October 2021 to June 2022, with funding from the Palestinian-German Science Bridge (PGSB).

Key words: γ-secretase, presenilin-1, p-Benzoyl-L-phenylalanine.

Table of Contents

List of Tables

List of Figures

List of Definitions of Abbreviations

Abbreviations	Title
Å resolution	Ångström-resolution
aaRS	Aminoacyl-tRNA synthetase
AD	Alzheimer’s disease
AICD	Non-pathogenic APP intracellular domain
APH-1	Anterior pharynx-defective 1
APP	Amyloid precursor protein
Aβ	Amyloid beta peptide
Aβ40	Aβ isoform 40 residues long
Aβ42	Aβ isoform 42 residues long
BACE1	β-Secretase
bp	Base pair
Bpa-RS	*Methanococcus jannaschii* tyrosyl-tRNA synthetase, Bpa-synthetase
C99	Membrane-bound fragment
CFPS	Cell-Free Protein Synthesis
CNS	Central Nervous System
E. coli	Escherichia coli (E. coli)
eGFP	Enhanced green fluorescent protein
FAD	Familial Alzheimer's disease

FAD	Familial Alzheimer's Disease
FRET	Förster Resonance Energy Transfer
g	Grams
GCE	Genetic code expansion
GS	γ-Secretase
GSIs	γ-secretase inhibitors
GSMs	γ-secretase modulators
IMAC	Immobilized Metal Affinity Chromatography
IPTG	Isopropyl-β-D-1-thiogalactopyranoside
KPI	Potassium Phosphate Buffer
LB	Lysogeny broth
MgOAc	Magnesium acetate
MS	Mass spectrometry
NaOAc	Sodium acetate
ncAA	Non-canonical amino acid
NCT	Nicastrin
NFT	Neurofibrillary tangles
Ni-NTA	Nickel-nitrilotriacetic acid
O. D	Optical density
pBpa	p-Benzoyl-L-phenylalanine

PEN-2	Presenilin enhancer 2
PS	Presenilin
PS CTF	PS1 carboxyl-terminal fragment
PS NTF	PS1 amino-terminal fragment
PS1	Presenilin
sAPPβ	Soluble fragment and
SDS-PAGE	Sodium Dodecyl Sulfate Polyacrylamide Gel Electrophoresis
SDS-PAGE	Sodium dodecyl-sulfate polyacrylamide gel electrophoresis
TB	Traffic Broth media
TEMED	N, N, N′, N′-Tetramethylethylenediamine
TEV protease	Tobacco Etch Virus protease
TM	Transmembrane
$tRNA_{CUA}^{opt}$	*Methanococcus jannaschii* tyrosyl-tRNA
UAA	Unnatural amino acid
UAG	Amber codon
UV	Ultraviolet light

Chapter One: Introduction

This chapter introduces the research topic and provides the necessary background information to understand the study and its key aspects. Also, it defines the research objectives. This section is laying the groundwork for an obvious understating of the scope and importance of the study. This chapter will address the research problem, the study's objective, the specific goals, research questions, and the hypotheses that underpin this research. The significance and impact of research will be highlighted. Key terminology will be defined.

The topic in general term

Designing a small-scale cell-free protein synthesis system (CFPS) of protein synthesis for a photo reactive amino acid site- specifically incorporated, namely p-Benzoyl-L-phenylalanine (pBpa), at presenilin-1 (PS1) sequence.

Briefly description of the research topic:

Site-specific incorporation of unnatural amino acids into proteins through CFPS is an efficient and less expensive means which enables precise protein structural modifications for a range of scientific purposes, among them the study of protein function and interactions (Majekodunmi et al., 2024). Recent studies show many advantages of CFPS compared with in vivo systems. The CFPS is a fast method that yields recombinant protein due to the open environment, which means first, to get high-throughput protein, there is no need to clone the gene and to do many steps that consume the time. Second, fast expression of recombinant proteins in just a few hours using the appropriate DNA templates. Third, there is no need to think about the transportation of the unnatural amino acids (UAA) and their cytotoxicity (L. Zhang et al., 2021). Moreover, CFPS, especially Escherichia coli (E. coli) systems for the recombinant proteins, have more advantages over in vivo systems (Smolskaya et al., 2020).

In this study, a CFPS system will be designed to introduce pBpa, which is a photoreactive amino acid called at a specific site of PS1 using the expanded genetic code. This approach requires a unique codon (the amber codon), which is the least-used stop codon in E. coli. UAA is reassigned at the amber codon using an engineered pair of orthogonal aminoacyl-tRNA synthetase (aa-RS) and its corresponding tRNA. This aa-RS and its tRNA pair were designed to precisely identify and attach UAA to tRNA, that subsequently incorporates the UAA at the site of amber codon during the translation process. The final expected product is an insoluble, full-length PS1-mutant, that has photocross-linker UAA, pBpa.

CFPS systems of UAAs site-specific incorporation face the problem of the endogenous competition of the natural amino acids because the rate of the incorporation of UAAs charged orthogonal aa-RS is slow, leading to disincorporation of the endogenous aa-RS and resulting in a truncated protein because the codon is recognized as a stop signal in the translation process (Cui et al., 2020).

When the unnatural amino acid pBpa site-specific is incorporated successfully into recombinant proteins, it will help photocross-linking which studies and helps in mapping and identifying the structure of proteins like γ-secretase (GS) and its subunits (Hino et al., 2005). GS plays a key role in producing the amyloid beta-protein (Aβ) by cleaving the amyloid precursor protein (APP) (Zhang et al., 2023). A decrease in the GS activity leads to Aβ accumulation in the brain, a hallmark for Alzheimer's disease (AD) (H. Zhang et al., 2021), this highlight the importance of studying this enzyme's complex and structure. Photocrosslinking can be combined with mass spectrometry (MS) and other techniques of structural biology to obtain a deeper understanding of the enzyme’s complex, function, and potential drug targets in the enzyme (Leitner et al., 2016).

The research problem

The main challenge of this study is to successfully establish a CFPS system capable of incorporating a photo-crosslinker unnatural amino acid, pBpa, at the 190th amino acid position of PS1 (as a test case) using a specific orthogonal pair of aa-RS and its corresponding tRNA (Bpa-RS and $tRNA_{CUA}^{opt}$), alongside with the strategy of using an amber codon to mediate the site-specific introduction of UAA into the protein sequence within an E. coli lysate. So the research questions are:

1. Is it possible for Bpa-RS and its $tRNA_{CUA}^{opt}$ to effectively facilitate the pBpa incorporation into the target site of the PS1 sequence?
2. How effective is the protein expression system when using the photocross-linker UAA to produce full-length PS1?
3. What is the efficiency of the IMAC purification protocol to isolate pure Bpa-RS?
4. How effective is the phenol-chloroform extraction method to isolate tRNA?

Objectives of the study

Many goals have to be achieved to solve the study's problem.

1. Gene conformation and testing the transformation efficiency of plasmids

- Confirm the presence of the essential genes for the experiments (Bpa-RS, $tRNA_{CUA}^{opt}$, PS1-N190-amber, and GFP gene) within their plasmids.
- Test the effectiveness of the plasmid transformation on their host cells.
- Perform double digestion using the appropriate restriction enzymes, followed by agarose gel electrophoresis to verify the plasmid content.

2. Plasmid extraction and the alcohol precipitation of DNA

- Extract the target plasmids using the extraction protocols of the Plasmid Kit Jel Gene mini prep and Plasmid Kit Jel Gene maxi prep.
- Determine the concentration of DNA using a nanodrop device (A260/A280 ratio).

- Concentrate the DNA using the alcohol precipitation protocol.

3. Expression and isolatation of tRNA

- Induce the expression of tRNA by 0.02% arabinose and express within BL21 Star™ (DE3) E. coli.
- Isolate tRNA by the phenol-chloroform extraction method.
- Determine the concentration of tRNA using a nanodrop device (A260/A280 ratio).
- Conduct urea polyacrylamide gel electrophoresis (UREA-PAGE) to confirm the purity of tRNA.

4. Induction and expression of target proteins

- Express and induce the proteins under the study (Bpa-RS and TEV protease).

5. Ni-Indigo purification and dialysis for proteins under the study

- Purify Bpa-RS and TEV protease by IMAC technique.
- Perform dialysis with the appropriate solutions, pH, and temperature conditions.

6. Detection of protein presence and purity

- Conduct SDS-PAGE to determine the presence and purity of protein.
- Follow up with western blotting and Coomassie blue staining.

7. Characterization of CFPS for the production of pBpa Photo-labeled PS1

- Construct an effective CFPS system for the synthesis of PS1 mutant.
- Apply a continuous exchange (dialysis) approach for CFPS.
- Evaluate the performance of three different setups: The pET15b-PS1 plasmid with orthogonal Bpa-RS and its corresponding tRNA, the pET15b-PS1-N190 with orthogonal Bpa-RS and its corresponding tRNA, and a control group.
- Analyze the expression of protein using SDS-PAGE and western blot

8. Optimization of CFPS for production of pBpa Photo labeled PS1 and quantification by eGFP

- Determine the optimal plasmid amount for expression using the pET28a-GfP-PS1 plasmid and test different plasmid concentrations ranging between 0.6 and 1.5 µg.
- Set up a calibration curve for eGFP quantification using 10-fold serial dilutions of eGFP.
- Use a fluorescence plate reader to determine the fluorescence intensity of the samples of eGFP.

Hypothesis

This study hypothesizes that pure Bpa-RS is expected to be obtained after applying the IMAC purification and following the protein expression protocol. the suppressor tRNA is also expected to be isolated after using the phenol-chloroform extraction method.

Moreover, the site-specific incorporation of pBpa at the 190^{th} site of the PS1 sequence, using the desired mutant of Bpa-RS and its tRNA pair into E. coli cell lysates, will successfully produce an insoluble, pure, folded, and full-length PS1 mutant with the photocross-linker unnatural amino acid, pBpa.

Briefly description of Methodology:

Both quantitative and qualitative research methodologies will be followed in this study. All methods are needed to achieve the study objectives described in the methodology chapter. In summary, the methods will be used to achieve the study objectives.

1. CFPS reaction in a continuous exchange (Dialysis):

The simplicity of the dialysis E. coli CFPS system makes them the most commonly used for protein production that contains the essential components of the translation machinery.

2. Phenol/chloroform RNA extraction method

To separate and purify RNA from BL21 Star™ (DE3) using this method by adding acidic phenol to a sample containing the nucleic acid.

3. sodium dodecyl-sulfate polyacrylamide gel electrophoresis (SDS-PAGE)

The separation of proteins will have been done based on proteins' molecular weight.

4. IMAC purification of His-tagged proteins

After the expression of the protein in Escherichia coli, a technique gives high purity for the protein by binding to the IMAC resin.

5. Western blotting

Technique for interest protein detection using specific antibodies and analysis after transfer of the denatured proteins by SDS-PAGE into a Polyvinylidene fluoride (PVDF) membrane.

6. Electrophoresis

A method used to separate DNA and RNA with different sizes.

For the results, they will be analyzed by

1. Western blot analysis using specific antibodies for detection of the protein of interest. The analysis of data is quite easy by comparing the bands of protein to molecular weight markers depending on size, and the target protein could be known according to its size. The bands with unexpected sizes or multiple bands for one sample are considered as wrong data. The intensity of the band shows the amount of protein.
2. Coomassie brilliant blue stain to make the proteins separated by SDS-PAGE visible as bands, and according to the molecular weight markers used in the SDS-PAGE, the protein under interest will be detected, and this method helps to examine the purity level of the protein after IMAC.

3. Gel electrophoresis technique, which uses an RNA or DNA ladder containing RNA or DNA fragments of known lengths, the samples of interest could be known.

Key Terminologies

Amyloid Plaques:

Abnormal accumulation of amyloid-beta (Aβ) protein that aggregates between neurons in the brain interferes with communication and harms cells.

γ-secretase (GS) complex:

An intramembrane multi-subunit protease complex which is highly conserved and responsible for integral membrane protein cleavage that influences many biological processes.

Notch Signaling Pathway:

A cell signaling mechanism that controls cell proliferation, differentiation, and survival in multicellular organisms. Notch signaling impacts various developmental and adult processes, such as neurogenesis.

Alcadein:

A protein played in neuronal functioning and development. GS processes this protein. It plays a role in synaptic function and is associated with neurodegenerative disorders.

TREM2 (Triggering Receptor Expressed on Myeloid Cells 2):

A receptor implicated in immunological responses, specifically microglial activation, which has been connected to many neuroinflammatory conditions and AD. TREM2 is processed by GS, which influences interactions of neuroimmune.

Tyrosinase:

An enzyme plays a role in the production of pigment, specifically melanin. GS processes tyrosinase. This affects pigmentation and associated biological functions.

Amyloid Precursor Protein (APP):

A transmembrane protein cleaved by GS. After cleavage, it produces amyloid beta (Aβ) peptides. They aggregate to form plaques in AD.

Aβ40 and Aβ42 amyloid beta:

Amyloid beta peptide variants, which are produced by cleavage of GS. Aβ42 is more likely to aggregate, and this leads to formation the amyloid plaques, which is a hallmark of AD.

Non-Amyloidogenic Pathway:

One of the APP processing pathways that prevents the amyloid beta peptide formation. α-secretase cleaves APP to create sAPPα and C83 in this pathway, which GS then processes into P3 peptides and the APP intracellular domain (AICD).

Amyloidogenic Pathway:

A APP processing pathway where β-secretase (BACE1) breaks down APP, producing sAPPβ and C99. sAPPβ and C99 are subsequently cleaved by GS to produce Aβ peptide variants, such as the pathogenic Aβ42, which is linked to AD.

α-Secretase:

An enzyme breaks down APP in the non-amyloidogenic pathway to create sAPPα and C83.

β-Secretase:

In the amyloidogenic pathway, β-Secretase is an enzyme that cleaves APP, producing soluble APPβ and C99. APPβ and C99 are further broken down by GS. This produce Aβ peptides.

Presenilin 1 (PS1):

A central catalytic unit of the GS complex. This unit is believed to be the responsible for the cleavage of APP and other substrates.

AICD (APP Intracellular Domain):

A fragment generated from APP cleavage by GS. AICD has roles in gene regulation and cellular signaling.

Presenilin Enhancer-2 (Pen-2), Nicastrin (NCT), anterior pharynx-defective 1 (Aph-1):

GS complex's components that aid in its formation and function. Stability of the complex and its activity may be affected by alteration in any of these subunits.

Neurotoxicity:

Toxic effects on neuron are often induced by the buildup of Aβ peptides in AD. This leads to damage and death to neurons.

Photoaffinity Labeling:

A method employs chemical probes to bind to a target protein specifically. A photoactive group forms a covalent bond with the target protein upon exposure to UV light, allowing analysis and identification of the target protein.

Unnatural Amino Acids (UAAs):

Synthetic amino acids with a chemical structure distinct from the 20 natural amino acids.

pBpa (p-benzoyl-p-phenylalanine):

An unnatural amino acid used in photo-crosslinking research.

Cryo-Electron Microscopy (Cryo-EM):

A technique that determines of the 3D structures of proteins and complexes at near-atomic resolution.

X-ray Crystallography:

A method used for determining the atomic structure of a protein by examining the X-rays diffraction pattern created when X-ray pass through a crystallized protein sample.

Mass Spectrometry:

An analytical technique used for determining an ion's mass-to-charge ratio.

Site-Directed Mutagenesis:

A method for studying the function of individual amino acids or protein domains by introducing specific changes into a gene sequence.

Genetic Code Expansion (GCE):

A technique of incorporating UAAs into proteins in order to extend the standard genetic code. It employs orthogonal aminoacyl-tRNA synthetase and tRNA pairs to insert UAAs at designated codons in the protein sequence.

Orthogonal Aminoacyl-tRNA Synthetase (aa-RS):

An engineered enzyme designed to identify and attach a particular unnatural amino acid (UAA) to its matching tRNA, enabling the UAA to be integrated into a protein at the target site.

Amber Stop Codon (UAG):

A termination codon (UAG) is typically employed to signal the end of protein synthesis.

Cell-Free Protein Synthesis (CFPS):

An in vitro protein production method and a controlled environment for protein expression and manipulation that employs the cellular machinery extracted from cells to produce proteins outside of a living organism.

Transcription and Translation:

The processes by which genetic information encoded in DNA is transformed into proteins. Transcription is the process of the synthesis of messenger RNA from DNA, while translation is the process which by which ribosomes synthesis of proteins from mRNA.

Chapter Two: Literature Review

Gamma-Secretase: A Crucial Intramembrane Protease

GS is a transmembrane enzyme, consists of PS1, nicastrin (NCT), anterior pharynx-defective 1 (APH-1) and presenilin enhancer 2 (PEN-2) (Kedia et al., 2021) **(Fig. 2.1)**. These components cross-regulate each other, and the absence of one destabilizes others and alters their cellular trafficking. The overexpression of all four components increases the activity of this enzyme (Zhang et al., 2014). The total size of the GS complexes is approximately 230 kDa, and the glycosylation mass of NCT ranges from 30 to 70 kDa (Zhang, Li, Xu, & Zhang, 2014).

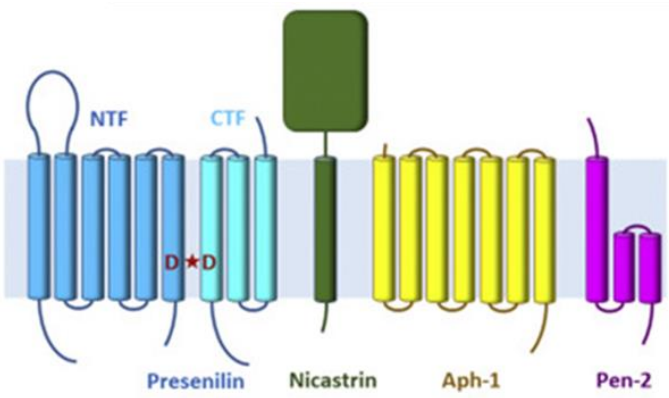

Figure 2. 1. Components of the GS complex and their membrane topology. (Modified from Wolfe & Miao, 2022).

PS1 is the core catalytic unit within the GS complex, pivotal in the cleaving of transmembrane proteins like APP and the Notch receptor (S. Zhang, Zhang, Cai, & Song, 2013). Mutations in PS1 are linked to onset forms of FAD at an early age (Berezovska et al., 2005). Such mutations typically alter the production of Aβ peptides, favoring the formation of the Aβ42 form (Verdile, Gandy, & Martins, 2007). Recent research suggests that PS1 serves a variety of functions, not all of which rely on the proteolytic activity of GS. These activities include roles in β-catenin signaling regulation, protein trafficking, calcium

homeostasis, and turnover, highlighting PS1 and GS as promising drug targets for AD and possibly other conditions (Oikawa & Walter, 2019).

This enzyme is a highly conserved intramembrane protease that participates in many critical biological activities through cleaving functionally important proteins (Fraering, 2007). GS is essential for the Notch receptor-mediated signaling pathway, which is important for regulating cell differentiation processes in all multicellular organisms, from embryogenesis through adulthood (van Tetering & Vooijs, 2011). GS also processes proteins such as alcadein, TREM2, and tyrosinase, each involved in many biological functions, including neural development, pigmentation, and immune response (Zhang et al., 2014).

GS contributes to APP processing. There are two main pathways for APP processing: The non-amyloidogenic pathway and the amyloidogenic pathway (Zhou et al., 2018) **(Fig. 2.2. A & B)**. In the non-amyloidogenic pathway, α-secretase cleaves APP initially, yielding sAPPα, a soluble fragment, and C83, a membrane-bound fragment (Chow et al., 2010). Subsequently, GS processes C83, generating P3 peptides and the non-pathogenic APP intracellular domain (AICD) (Urban et al., 2021) **(Fig. 2.2.A)**.

In contrast, in the amyloidogenic pathway, Aβ peptides are produced, which are associated with AD (Wang et al., 2017). APP is cleaved by β-secretase, producing sAPPβ, a soluble fragment, and C99, a membrane-bound fragment. Subsequently, GS cleaves C99 into various lengths of Aβ peptides (Aβ40, Aβ42, and others) and AICD **(Fig. 2.2.B)**.

While APP is necessary for neurons to develop, communicate, and maintain their health (Zhou et al., 2011), certain types of amyloid, especially Aβ42, can become harmful (Vadukul et al., 2017). Because Aβ42 is longer than the more common Aβ40 and tends to clump together, it is more toxic to the brain (Murphy & LeVine, 2010).

Normally, the brain has systems to remove excess amyloid and preserve balance (Tarasoff-Conway et al., 2015). In AD, these mechanisms malfunction, causing plaque to form. When Aβ42 builds up, it creates small aggregates called oligomers. These oligomers are thought to be extremely toxic because they interact with surrounding brain cells, reducing their functionality and accelerating the disease's progression. Eventually, these oligomers unite to form dense, insoluble plaques that impair cell communication, induce inflammation, and cause damage to cells (Roda et al., 2022).

Several pathological processes in AD are linked to the accumulation of Aβ42, including neurotoxicity, inflammatory responses, vascular damage, and the formation of amyloid plaques (Nasb et al., 2024). The amyloid plaques interfere with neuronal transmission and cause cognitive decline (Hampel et al., 2021).

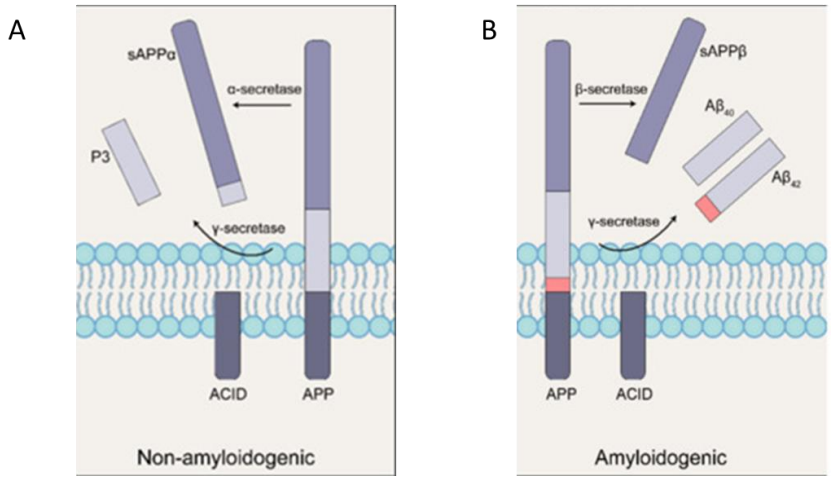

Figure. 2. 2. Two main pathways for APP processing:
(A) The non-amyloidogenic pathway. (B) The amyloidogenic pathway.
(Modified from Y. Zhao et al., 2022)

Integrating Site-Specific Incorporation of Unnatural Amino Acids with Genetic Code Expansion

Several techniques have been employed to study the molecular architecture of GS, including Cryo-EM (Yang et al., 2021) (Yang, Zhou, & Shi, 2017), X-ray crystallography, biochemical and biophysical methods (Wolfe, 2013), site-directed mutagenesis (Kornilova, Bihel, Das, & Wolfe, 2005), nuclear magnetic resonance (Li, Liew, Li, & Kang, 2016), spectroscopy (Li et al., 2016), and computational modeling and molecular dynamics simulations (Aguayo-Ortiz, Chávez-García, Straub, & Dominguez, 2017).

Chemical probes, particularly through photoaffinity labeling, allows for the site-specific tagging of proteins, is providing practical and valuable insights into the mechanistic and structural aspects of GS (Smith & Collins, 2015). A photoaffinity probe typically consists of three components: A ligand that binds to the target protein, a photoactive group which covalently reacts with the target upon UV irradiation, and a reporter that is used to isolate the target complex. The ligand guarantees specificity by identifying and binding to the active site or other region of the target protein. UV light activates the photoactive group, typically diazirine or benzophenone. This leads the group to form a covalent bond with nearby amino acid residues. Lastly, the reporter—such as a biotin or fluorescent tag, for example —allows the target protein and its interacting partners to be purified and analyzed afterward (Nie et al., 2020).

By coupling photoaffinity labeling with the incorporation of UAAs into proteins, researchers can create extremely specific probes to investigate GS (Smith & Collins, 2015). Moreover, the use of photoaffinity probes in combination with UAAs creates novel avenues for studying protein-protein interactions, protein conformational changes, and the effects of small molecules on enzyme activity (Smith & Collins, 2015). Recent advancements in mass

spectrometry (Li et al.) and other analytical methods have further expanded the capabilities of photoaffinity labeling, enabling the characterization of intricate protein complex and the high-resolution identification of labeled sites (Petrotchenko & Borchers, 2022).

Peter G. Schultz and his team successfully demonstrated that GCE for incorporating UAA could work efficiently in E. coli and eukaryotic cells. They incorporated successfully an UAA into a specific protein using the amber stop codon and an O-aaRS and its corresponding tRNA system. The technique has been further developed and widely applied in protein engineering, protein studies, biopharmaceutical development, and designing proteins with novel functions(Wang et al., 2001).

Unnatural Amino Acids

UAAs are artificial analogs of natural amino acids with special chemical characteristics that are not found in nature, such as fluorescent tags, reactive moieties, metal-binding sites, and photo-cross linkers (Guo & Cao, 2024). They play a crucial role in studying protein dynamics, interaction, and structure. This process aims to improve stability, increase therapeutic efficacy, alter catalytic activity, and reduce immunogenicity. They can be incorporated into proteins at desired positions, facilitating the production of proteins with novel functions and properties and the development of novel protein-based therapies (Lee et al., 2019; Young & Schultz, 2010).

The synthesis of some unnatural amino acids starts with a modification of the side chain or the backbone of a natural amino acid. Organic backbone blocks, like aldehydes, could serve as the starting point for the synthesis of new UAAs. The choice of the precursor depends on the structure and properties of the targeted UAA (Castro et al., 2023). For example, pBpa is a widely used UAA (Information, 2024) **(Fig. 2.3)**.

p-Benzoyl-L-phenylalanine (pBpa)

pBpa is synthesized by attaching a benzoyl group to the para position of L-phenylalanine. Through this modification, photo-crosslinkable properties were imparted to the resulting amino acid, pBpa (Kauer et al., 1986). With regard to photo-crosslinking research, this modification is essential because it enables pBpa to form covalent bonds with nearby molecules when exposed to UV light (Forné et al., 2012) **(Fig. 2.4)**. Umanah et al. incorporated successfully pBpa into G Protein-coupled Receptor. This strategy enables site-specific photo-crosslinking to investigate the receptor interactions and conformational changes. This approach offers valuable insights into G Protein-coupled Receptor structure and function (Umanah et al., 2009).

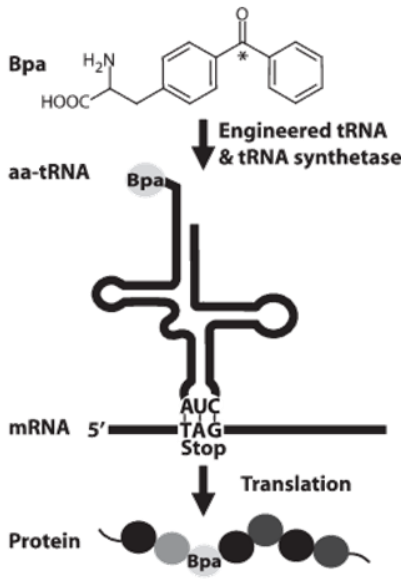

Figure 2.3. Photo-crosslinking with a genetically encoded unnatural amino acid.

The photo-crosslinkable amino acid pBpa, and how it incorporates in the amino acid sequence of protein using the GCE strategy.

(Modified from Forné et al., 2012).

Site-Specific Incorporation of Unnatural Amino Acids and Genetic Code Expansion

Site-specific incorporation of UAAs is a specialized method in protein engineering that enables the exact introduction of UAAs into particular sites within a protein's sequence. This technique allows the production of proteins with particular chemical or structural properties

for research and therapeutic applications. Moreover, this technique facilitates the study and manipulation of detailed aspects of protein function, structure, and interactions (Peeler & Mehl, 2012). GCE is employed to achieve this level of precision. GCE is a technique that directly enables the insertion of UAAs into proteins in cell-free systems or living organisms. This technique extends the genetic code to add new chemical properties to proteins at targeted sites (Guo & Cao, 2023).

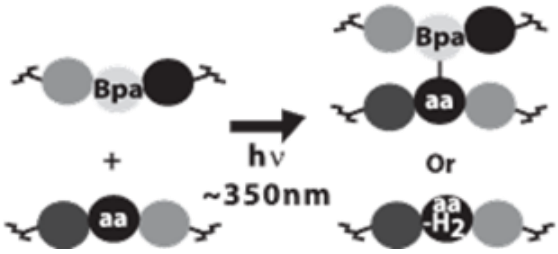

Figure 2.4. Photoactivation of Bpa by UV light.
(Modified from Forné et al., 2012).

GCE provides the essential framework and tools to incorporate UAAs at the target sites within proteins through several strategies, one of them is the amber suppression strategy. This is how this strategy works:

A. Orthogonal aa-RS and tRNA Pair

The development of an orthogonal aa-RS and tRNA pair is the foundation of GCE. The creation of an orthogonal aa-RS and tRNA allows UAAs to be precisely incorporated into proteins (Melnikov & Söll, 2019). *Methanocaldococcus jannaschii*, a thermophilic methanogenic archaean which thrives in extreme conditions, plays an important role in GCE by providing unique aa-RS and tRNA pairs (Wals & Ovaa, 2014). These orthogonal pairs are particularly designed to avoid cross-reacting with the native translation machinery of the host (Patel et al., 2024) **(Fig. 2.5)**.

In E. coli expression systems, the natural ability of Methanocaldococcus jannaschii to incorporate tyrosine at UAG codons is modified for the precise insertion of UAAs (Wals & Ovaa, 2014).

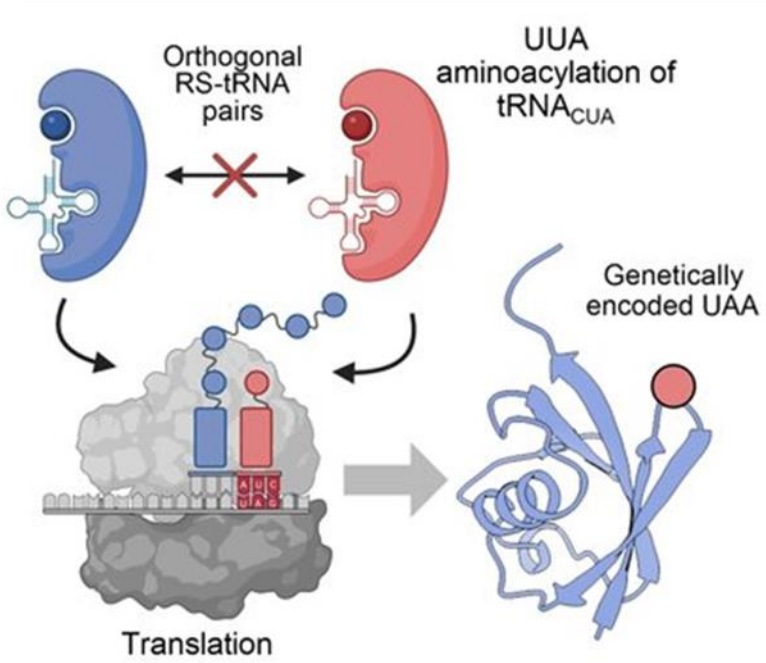

Figure 2.5. Genetic code expansion by orthogonal aa-RS /tRNA pairs. (Modified from Patel et al., 2024)

The components of this system consist of:

1. aa-RS: This specific enzyme is engineered to identify and attach a UAA to its appropriate tRNA. This enzyme is designed to avoid interaction with the host's endogenous amino acids through strategies like directed evolution **(Fig. 5)**. This ensures that aa-RS preferentially binds UAA, activates it, and does not interfere with natural amino acids that are needed by the host for protein synthesis (Lee et al., 2024) **(Fig. 2.5)**.

2. tRNA: This tRNA is made to be detected by the orthogonal aa-RS and to integrate the UAA at the target site in the protein, directed by its anticodon sequence (Kim et al., 2024) **(Fig. 2.5&2.6&2.7)**.

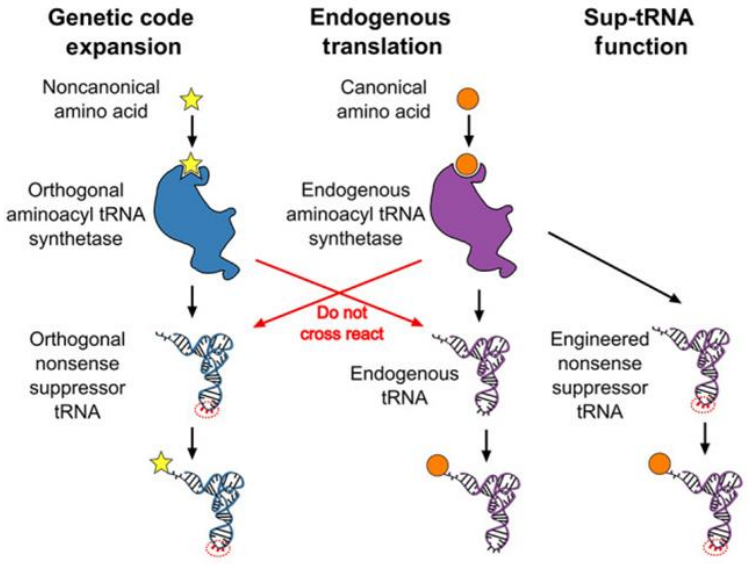

Figure 2.6. Genetic code expansion. (Modified from Porter et al., 2021).

B. Amber Stop Codon (UAG)

The optimal choice for GCE experiments is the amber stop codon (UAG), which is normally a signal for stopping protein synthesis (Nikić-Spiegel, 2020) and is less frequent compared to the other two stop codons (Belin & Puigbò, 2022). In GCE, the amber codon serves a different purpose (Nikić-Spiegel, 2020). Specifically, a mutation is induced at a specific site in the protein's DNA sequence to change a sense codon to an amber codon. When this amber codon is encountered, the orthogonal aa-RS/tRNA pair recognizes the UAG and incorporates the UAA instead of terminating translation. The result is a protein with the UAA inserted at the desired site (Porter et al., 2021) **(Fig. 2.5 to Fig. 2.8)**. The efficacy of genetic code expansion was improved, and the selectivity of structural modification of proteins was increased by using the amber codon strategy (Bartoschek et al., 2021).

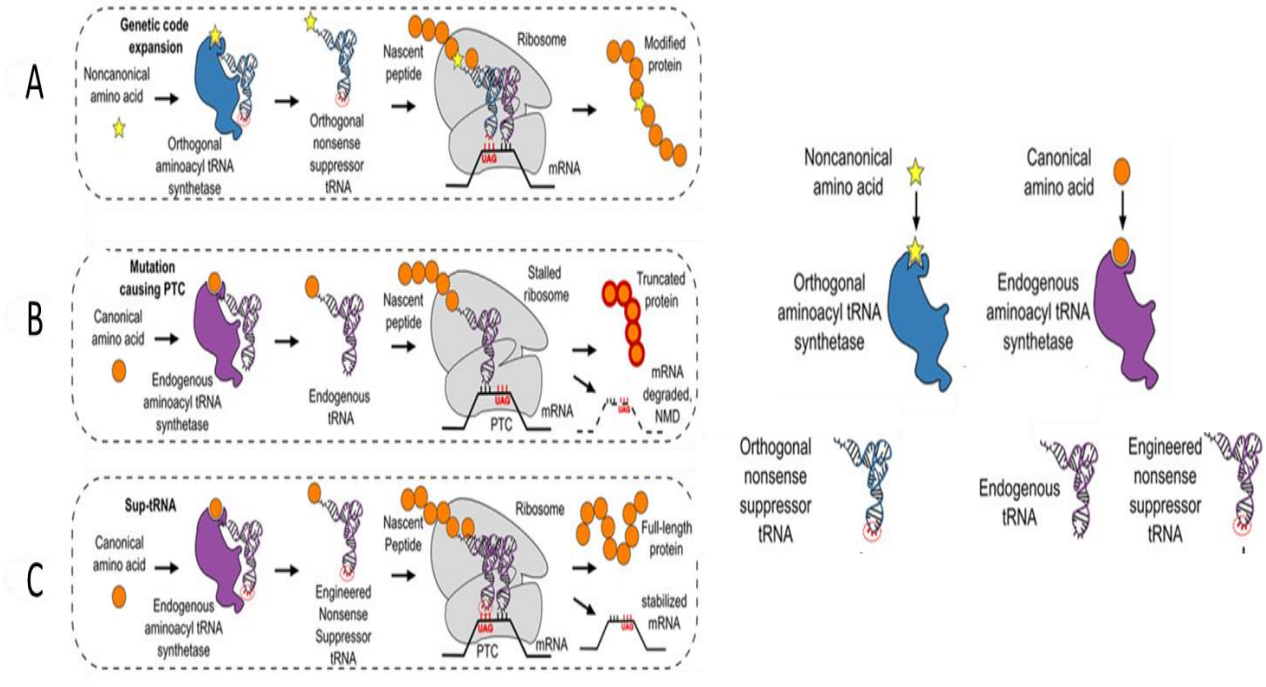

Figure 2.7. The applications of suppressor tRNAs and their function in translation.

(A) Mechanism of genetic code expansion.

(B) Premature termination codons (PTCs).

(C) Rescue of full-length protein expression.

(Modified from Porter et al., 2021).

C. In Vivo and in Vitro Applications of Genetic Code Expansion

GCE is a flexible technique that can be used in both living organisms and CFPS systems. The choice between in vivo and in vitro systems depends on the properties of the protein, UAA, and the particular application under study (Guo & Cao, 2024).

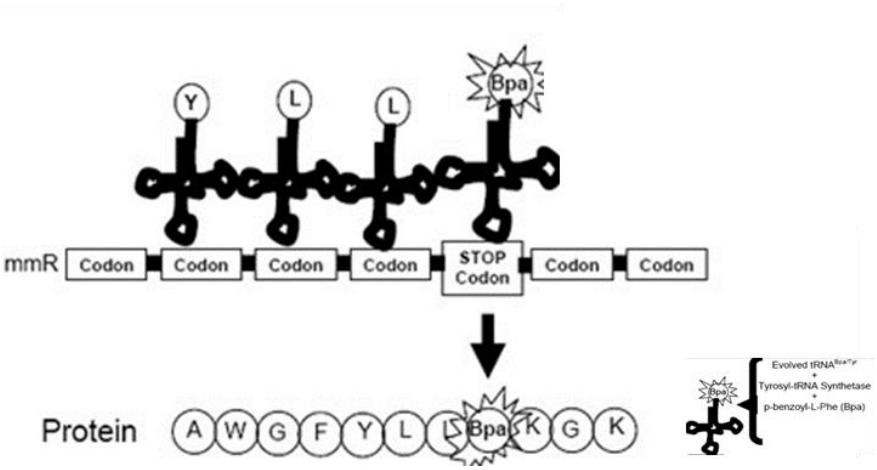

Figure 2.8. The site-specific incorporation of pBpa into Ste2p using an orthologous tRNA/aa-RS pair. (Modified from Umanah, 2009).

In Vivo Applications

UAA is incorporated into proteins during natural cellular processes using living organisms such as genetically modified E. coli. This approach utilizes the internal machinery of the host organism, which includes the aa-RS and tRNA pairs. These orthogonal components are engineered to be expressed in E. coli and other host organisms, and the UAAs are supplied to the media of cells. This engineering facilitates the GCE and allows for the study of protein structure, interactions, and function within a biological framework (Guo & Cao, 2024) **(Fig. 9).**

In Vitro Applications

In vitro applications utilize CFPS systems, where essential cellular components are extracted from organisms to carry out protein synthesis in a cell-free environment. CFPS systems offer a versatile and controlled environment which can directly manipulate the components of the transcription and translation processes.

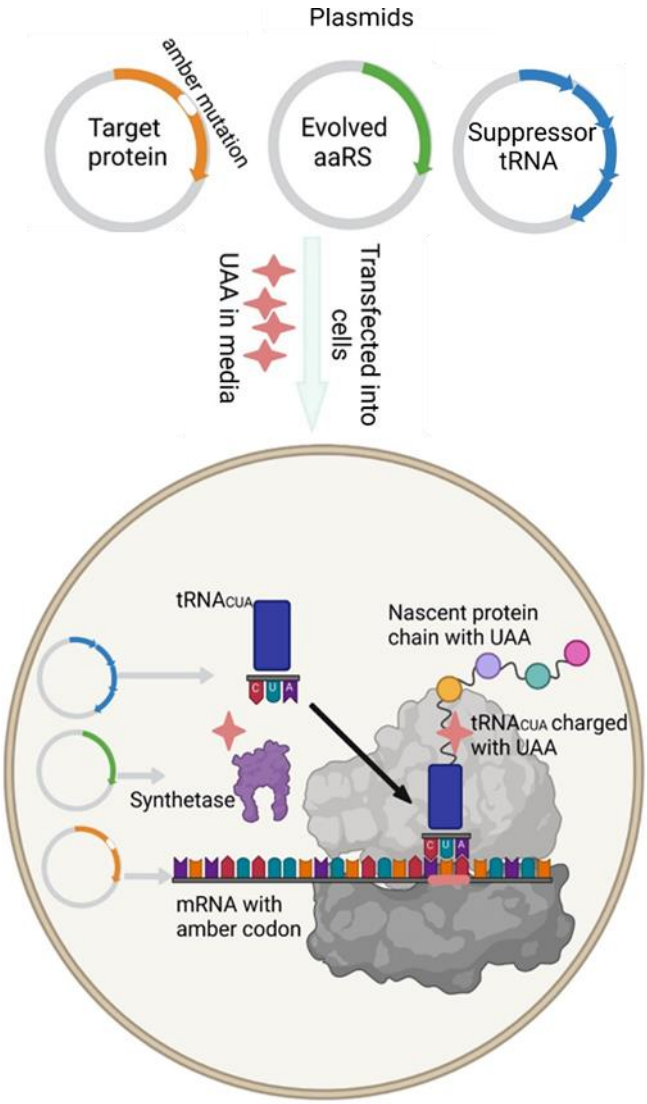

Figure 2.9**.** A schematic of UAA incorporation method. (Modified from Zhao & Liu, 2023).

This approach enables the rapid and scalable synthesis of proteins, including the integration of UAAs, without the limitations of in vivo systems. CFPS systems are particularly effective for conducting structural analyses and studying protein folding and function. Moreover, CFPS are also useful for producing toxic proteins and the proteins that are hard to express in an in vivo environment (Khambhati et al., 2019) **(Fig. 2.10)**.

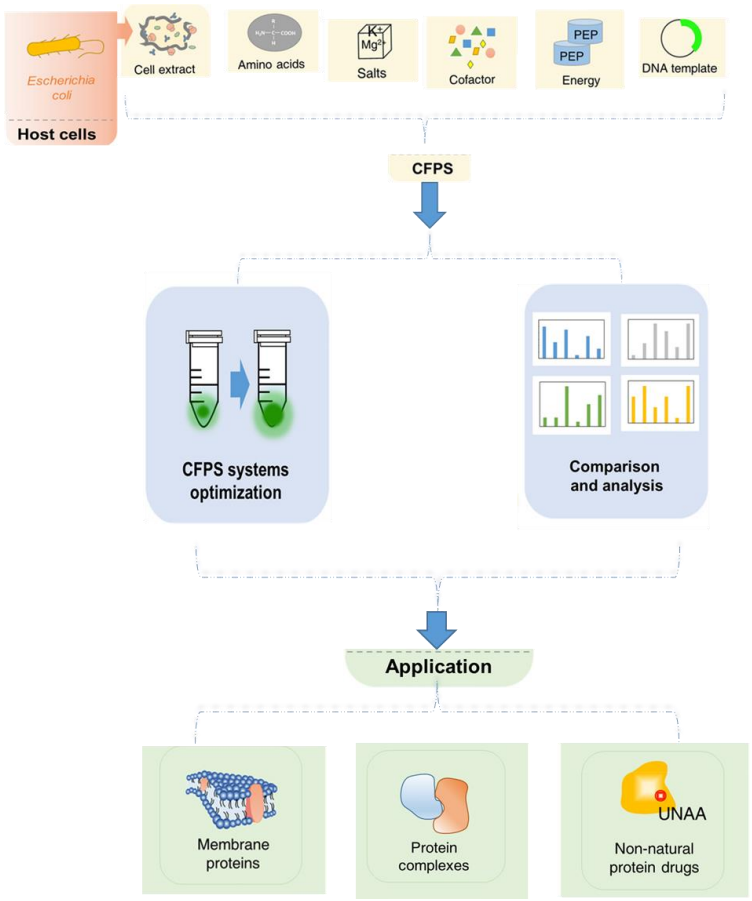

Figure 2.10. The CFPS system as a platform for basic scientific research, preliminary screening and related applications.(Modified from Zhang et al., 2021).

Cell-Free Protein Synthesis (CFPS) System

The CFPS system is an effective and flexible technology for protein production without the need for living cells. The essential cellular components are extracted from cells (E. coli) to produce the protein in vitro **(Fig. 2.10)** (Zhang et al., 2021).

1. Key Components of CFPS

This system utilizes the critical components of the cellular machinery to produce proteins directly in a test tube. The following are the key components of a CFPS system **(Fig. 2.10&2.11)**:

1. Cell Extract:

A CFPS system includes all factors necessary for transcription and translation, like tRNAs, ribosomes, and aa-RS.

2. Energy Source:

ATP and other energy sources are provided to power the protein synthesis process.

3. DNA or mRNA Template:

The genetic material encoding the target protein is supplied, enabling the CFPS system to synthesize the protein according to the given sequence.

4. Amino Acids:

All necessary amino acids for protein synthesis are present in the system, including any UAAs that are to be incorporated.

2. Advantages of CFPS

CFPS offers several benefits over in vivo expression, including rapid protein expression and production within a few hours (Gregorio et al., 2019). In theory, CFPS is an open system, which makes it easy to optimize the yield of protein and adjust the cellular components for the reaction. Moreover, there are no concerns about the toxicity, harmful effects on cell viability, or complications with the techniques of protein purification (Maharjan & Park, 2023). CFPS is an attractive choice over traditional cell-based systems, especially for the production of toxic or hard-to-express proteins (Dondapati et al., 2020) **(Table 1)**.

The technology could help in increasing the yield of proteins for screening assays and is vital for UAA incorporation in structural studies (Khambhati et al., 2019).

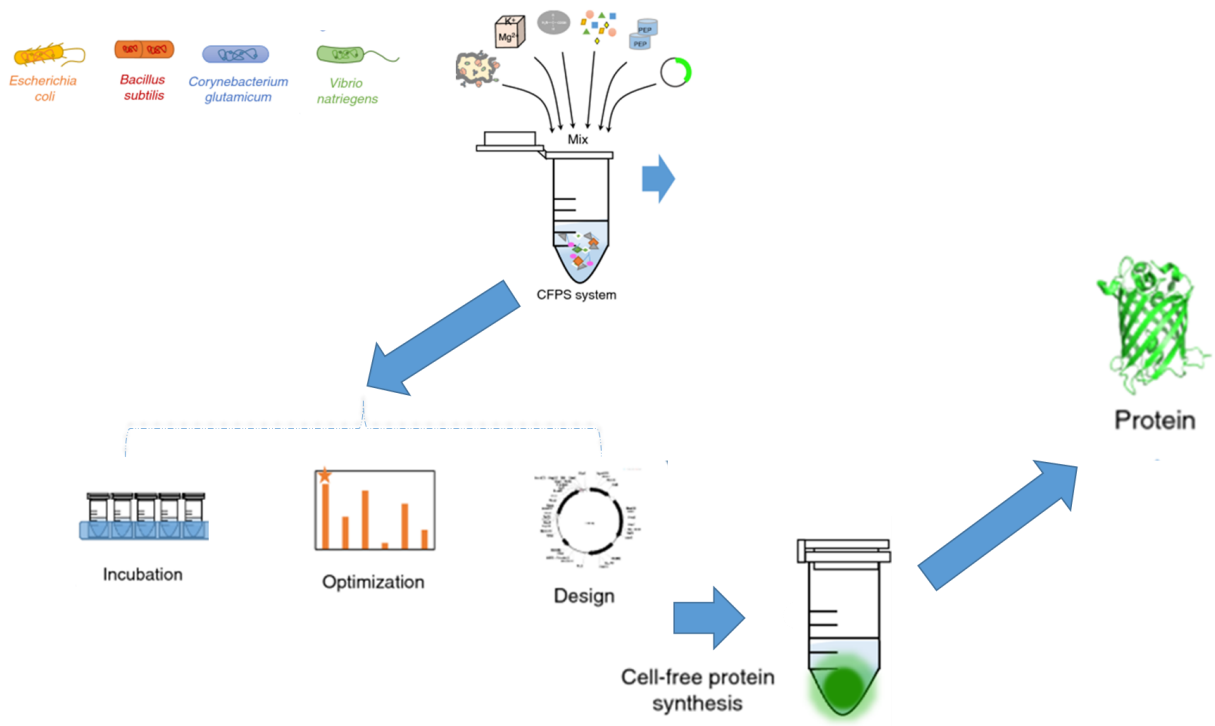

Figure 2.11. Cell-free protein synthesis systems.

(Modified from Zhang et al., 2021).

Table 2.1. The distinct advantages of CFPS compared to traditional cell-based systems (Modified from Dondapati et al., 2020).

Feature	Traditional Cell-Based System	CFPS (Cell-Free Protein Synthesis)
Efficiency	Often requires longer culture times for high yields.	Can achieve high expression levels in a shorter time frame.
Adaptability	Limited to specific cell types (E. coli, insect, mammalian).	Can use various cell extracts (e.g., wheat germ, rabbit reticulocytes) depending on needs.
Protein Quality	May involve more contaminants and complex purification.	Allows for the production of proteins with fewer contaminants and easier purification processes.

Chapter Three: Methodology

In this chapter, the methods that were applied to achieve the research goals will be detailed along with the experimental design and procedural steps.

1. Double digestion for verification of the plasmid

To confirm the presence of the target genes within the plasmids, double digestion and electrophoresis were conducted. The pattern of bands on the agarose gel verifies the presence of the desired genes within the plasmid. Details of each plasmid and its corresponding restriction enzymes used for the double digestion reaction are summarized in **Table 3.1**.

Each double digestion reaction had a volume of 20 µL, consisting of water, plasmid, reaction buffer, and restriction enzymes. The quantities of each component are outlined in **Table 3.2**. The reaction mixture was then incubated for 30 minutes at 37°C to ensure complete digestion (Sigma-Aldrich, 2024).

2. Transformation

All plasmids followed the same procedures for the transformation process. 100 µL of competent cells were mixed with 2 µL of plasmid. The mixture was incubated on ice for 30 minutes, then subjected to heat shock for 90 minutes at 42°C using a thermomixer. **Table 3.3** summarizes the host organism and its function for cloning or expression. 900 µl of Lysogeny broth (Albright) media were added to the transformed cells in the laminar flow hood. Then, the cells were incubated with shaking on the thermomixer for 1 h at 37°C and 700 rpm, allowing the recovery and expression of the plasmid (Biolabs, 2012). Subsequently, 100 µl of the mixture were plated on agar plates with appropriate antibiotics, as summarized in **Table 3. 4**. The plates were incubated overnight at 37°C, and the development of colonies was monitored.

Table 3.1. The plasmid and the restriction enzymes used for the double digestion.

	Plasmid	Restriction enzyme
1	pET2Vb-TEV-Bpa-RS	XhoI and NdeI
2	pETVOL-tRNA$_{CUA}^{opt}$	BamH1 and Nco1
3	pET15b-PS1-N190	Xhol and Nde1
4	pET28aGFP-PS1	NdeI and NcoI
5	pET15b-PS1	Xhol and Nde1

3. Alcohol precipitation of DNA and RNA

To concentrate the DNA and RNA, alcohol precipitation was used (Protocols.io, n.d.). Initially, 1/10 volume of cold 3 M sodium acetate (pH = 5.2), previously stored at -20°C for 30 minutes, was added. Then, 2 volumes of cold 100% ethanol were added and mixed before being stored at -80°C overnight. This was followed by thawing and centrifuging at maximum speed in a microcentrifuge at 4°C for 20 minutes.

Table 3.2. The components and amounts for the double digestion reaction.

	The component	The amount
1	Plasmid	1 µL
2	Restriction enzyme (1st)	0.5 µL
3	Restriction enzyme (2nd)	0.5 µL
4	Reaction buffer (10x Fast Digest Green Buffer)	2 µL
5	H_2O	16 µL

70% cold alcohol was employed to wash the pellet, followed by centrifugation at maximum speed in a microcentrifuge at 4°C for 20 minutes. Then, the pellet was washed with 100% cold alcohol. After air-drying for 2 minutes at room temperature, the DNA was suspended in MilliQ water using a vortex and then spun down (Protocols.io, n.d.).

Table 3.3. The host organism and their function for cloning or expression.

	Type of cells	Its function
E. Coli	Top 10	Cloning hosts
	BL21γ::DE3	Expression hosts for Bpa-RS
	BL21 Star™ (DE3)	Expression hosts for tRNA
	BL21 DE3 RIL	Expression hosts for TEV

4. The extraction of plasmid

For the extraction of plasmids, one or more of those colonies was selected and inoculated into either 4 mL or 1 L of LB media, as determined by the extraction protocol that was used. A 1:1000 dilution of the appropriate antibiotic relative to the volume of media was added. Then, the inoculated cultures were incubated overnight at 37°C with shaking. The extraction method followed the protocols provided in the user guide: GeneJET Plasmid Miniprep Kit, K0502 (Scientific, 2024b) and the user guide: GeneJET Plasmid Maxiprep Kit, K0491 (Scientific, 2024a). The concentration of DNA and RNA samples was measured using a NanoDrop spectrophotometer (A260/A280 ratio), and the extracted DNA and RNA were stored at -80°C for further tests.

5. Induction and expression of tRNA

To express tRNA, LB-T media and Z media were used to prepare the pre- and main-culture media, respectively (Kiyoshi Ozawa & Choy Theng Loh, 2014). LB-T media is comprised of 10 g/L tryptone, 5 g/L yeast extract, 5 g/L sodium chloride, 2.5 ml/L of 1 M sodium hydroxide and 0.5 mg/L thymine. While Z media consisted of 165 mM potassium dihydrogen phosphate, 664 mM dipotassium hydrogen phosphate and 40 g/L yeast extract (Kiyoshi Ozawa & Choy Theng Loh, 2014).

Table 3.4. The name of the protein or polypeptide, bacterial expression vector, gene of interest, vector name, bacterial resistance, and its concentration.

Name of Protein\ Polypeptide	Bacterial expression vector	Gene of interest	Vector name	Bacterial resistance (control) and its concentration
Bpa synthetase	pET2b-TEV-Bpa-RS	Bpa-RS	pET2b	Kanamycin (50 mg/mL)
$tRNA_{CUA}^{opt}$	pEVOL- $tRNA_{CUA}^{opt}$	$tRNA_{CUA}^{opt}$	pEVOL	Chloramphenicol (30 mg/mL)
TEV Protease	pRK93-TEV	TEV Protease	pRK93	Ampicillin (200 mg/mL) and Chloramphenicol (30 mg/mL)
GFP-PS1	pET28a-GfP-PS1	GFP	pET28a	Kanamycin (50 mg/mL)
Wild PS1	pET15b-PS1	PS1	pET15b	Ampicillin (200 mg/mL)
PS1 mutant	pET15b-PS1-N190X	PS1-n190-amber	pET15b	Ampicillin (200 mg/mL)

Following the successful transformation, one colony of BL21 Star™ (DE3) E. coli was inoculated in 4 mL of LB-T media with 0.4 µL of 30 mg/mL chloramphenicol and cultivated overnight at 37°C and 200 rpm shaking (Kiyoshi Ozawa & Choy Theng Loh, 2014).

The main culture was prepared by inoculating 1% of the pre-culture into fresh Z media with the addition of 2 M glucose, 1 mg/mL thiamine and a 1:1000 dilution of 30 mg/mL chloramphenicol. The culture was incubated at 37°C and 120 rpm shaking for 4 h (Kiyoshi Ozawa & Choy Theng Loh, 2014).

Table 3.5. The volume ratios of Bpa-RS to TEV protease that were used to test the TEV protease protein activity.

No.	Volume Ratio of Bpa-RS: TEV protease	Bpa-RS (23.05 mg) (μL)	TEV protease (3.55 mg) (μL)
1	1:1	3	3
2	1:2		6
3	1:3		9
4	1:4		12
5	1:5		15
6	1:0	15	0
7	0:1	0	15

When the optical density (O.D.) at 600 nm of the cells reached 0.5, the expression of tRNA was induced by adding 0.02% arabinose, followed by incubation at 37°C and 200 rpm for 4 h. The media was then centrifuged at 5000 xg for 25 minutes at 4°C and the pellet was collected and stored at -80°C (K. Ozawa & C. T. Loh, 2014).

Table 3.6. The components of the inhibitor cocktail.

Inhibitor cocktail	Working concertation	Dilution 1000X
E64	1uM	0.001
Pepstain A	1uM	0.01
Leupeptin	1uM	0.01
AEBSF hydrochloride (500 mg)	1mM	0.001
PMSF	1mM	0.01
Benzamine	1mM	

6. <u>The phenol-chloroform extraction for tRNA</u>

The extraction of tRNA was done following the protocol described in (Avcilar-Kucukgoze et al., 2020). After the thawing of cells, they were suspended in 0.9% NaCl, then collected by centrifugation for 15 minutes at 5,000 x g at 4°C. The pellet was collected and disrupted by a

mortar and pestle after being frozen in liquid nitrogen. During the disruption process, 10 mL of two solutions were added: a 50 mM sodium acetate (NaOAc) solution at pH=5 and a 10 mM magnesium acetate (MgOAc) solution at pH=5 (Avcilar-Kucukgoze et al., 2020).

Before this extraction process, acidic phenol was prepared by warming the phenol to room temperature and then melting it at 68℃. After that, 0.1% w/v 8-hydroxyquinoline was added to the phenol. A solution with a ratio of 25:24:1 of phenol, chloroform, and isoamyl alcohol was prepared and added in a ratio of 1:4 to the weight of the opened cells. The mixture was shaken for 1 minute, then centrifuged at 5,000 xg for 15 minutes at 4℃. The supernatant was saved for the next steps of the tRNA extraction (Avcilar-Kucukgoze et al., 2020). After that, 20.8 µl of 5 M NaCl and 1 volume of isopropanol were added to the collected supernatant to precipitate nucleic acids. After being stored for 30 minutes at room temperature, the mixture was centrifuged at 14,500 xg for 15 minutes at -20℃. The nucleic acid pellet was washed with cold 70% ethanol, then 100% ethanol, followed by centrifugation at 4000 xg for 20 minutes at -20℃. The nucleic acid pellet was air-dried for 5 to 10 minutes (Avcilar-Kucukgoze et al., 2020).

Table 3.7. The components of the feeding mix buffer and their stock and final concentrations for CFPS reaction of the three groups: the pET15b-PS1 plasmid with orthogonal Bpa-RS and its corresponding tRNA, the pET15b-PS1-N190 with orthogonal Bpa-RS and its corresponding tRNA, and the control group.

Component	Stock concentration	Final concentration
Tris-acetate, pH 8.2	1 M	10 mM
Magnesium acetate	1 M	14 mM
Potassium acetate	10 M	60 mM
DTT	1 M	0.5 mM
H2O		872.1 µL

To remove rRNA, the pellet was resuspended in 10 mL of cold 1 M NaCl, vortexed, and then centrifuged at 9,500 xg for 20 minutes at 4°C. The supernatant was collected, and to

precipitate the remaining nucleic acids (including DNA and tRNA), two volumes of cold ethanol were added to the supernatant, followed by 30 minutes of incubation at -20°C. The mixture was then centrifuged at 14,500 xg for 5 minutes at -4°C. The pellet was washed with cold 70% ethanol, followed by a wash with cold 100% ethanol, and then allowed to air-dry for 5 to 10 minutes (Avcilar-Kucukgoze et al., 2020).

Table 3.8. The components of the feeding mix and their stock and final concentrations for CFPS reaction of the three groups: the pET15b-PS1 plasmid with orthogonal Bpa-RS and its corresponding tRNA, the pET15b-PS1-N190 with orthogonal Bpa-RS and its corresponding tRNA, and the control group.

Component	Stock concentration	Final concentration\ volume
Master Mix		476.21µL
Feeding mix buffer	1X	0.35X
Amino acid mix	40 mg/mL	0.5 mg/mL
H2O		531.79 µL

To ensure the removal of DNA, the pellet was dissolved in 83.11 µL of 0.3 M NaOAc, pH 5.0. Then, 47.22 µL of cold isopropanol was added to the nucleic acid solution and incubated for 10 minutes at -20°C. The supernatant was then collected after centrifugation at 14,500 xg for 5 minutes at -20°C (Avcilar-Kucukgoze et al., 2020). For the final precipitation of tRNAs, 31.94 µL of cold water-isopropanol (1.00:0.95) solution were added to the supernatant and incubated for 30 minutes at -20°C. The suspension was then centrifuged at 14,500 xg for 15 minutes at 4°C. The pellet was washed with cold 70% ethanol and then allowed to air-dry for 5 to 10 minutes. Finally, the pellet was dissolved in 50 µL of DEPC-treated water and stored at -80°C (Avcilar-Kucukgoze et al., 2020).

7. UV-Vis Spectrophotometric Measurement Using Nanodrop (A260/A280 ratio)

The ratio of A260/A280 at wavelength 260 nm was used to determine the purity of RNA, and the protein concentration was measured at 280 nm ((NEB), n.d.). The measurements for both

RNA purity and protein concentration were facilitated by the software (Nanodrop 2000/2000c).

8. Gel electrophoresis technique

The gel electrophoresis technique is a method used to separate DNA and RNA based on size. In order to conduct gel electrophoresis, the extracted tRNA and the mixture from the double digestion, which was incubated for 30 minutes at 37°C, need to be mixed with 6x loading buffer, then heated for 2 minutes at 95°C (Lee et al., 2012).

Table 3.9. The components of the master mix buffer and their stock and final concentrations for CFPS reaction of the three groups: the pET15b-PS1 plasmid with orthogonal Bpa-RS and its corresponding tRNA, the pET15b-PS1-N190 with orthogonal Bpa-RS and its corresponding tRNA, and the control group.

Component	Stock concentration	Final concentration
6 Amino acid mix	16.7 mM	1 mM
Amino acid mix	25 mM	0.5 mM
Li+,K+ ACP	1M	20 mM
PEP	1M	20 mM
75X NTP mix	90 mM ATP; 60 mM G/C/UTP	1.2 mM ATP; 0.8 mM G/C/UTP
DTT	500 mM	2 mM
Folinic acid (Ca2+)	10 mg/mL	0.1 mg/mL
Complete protease inhibitor	100 X	1X
HEPEA/EDTA buffer	24 X	1 X
Magnesium acetate	1 M	16 mM
Potassium acetate	4 M	270 mM
PEG 8000	40% (w/v)	2% (w/v)
Sodium Azide	10% (w/v)	0.05% (w/v)
H2O		54.4 µL

A 1% agarose gel was prepared for electrophoresis by dissolving agarose in 50 mL of 1X TAE. The 1X TAE buffer was prepared using the 50X TAE stock solution, which is

composed of 242 g of Tris base, 100 mL of 0.5 mM EDTA, and 57.1 mL of glacial acetic acid, adjusted to pH 6.1 (Scientific, n.d.). To enhance the visualization of the bands, 2.5 µl of Gel Red dye were added to the gel solution. The resultant mixture was then loaded into wells of gel, alongside a 1 KB ladder as a molecular marker.

A 1X TAE running buffer was used to conduct electrophoresis for 30 minutes at 180 volts, allowing the proper migration of DNA or RNA fragments (Scientific, n.d.). After electrophoresis, the Bio-Rad ChemiDoc Imaging System, which was operated with Image Lab Touch software, was used to visualize the DNA bands and analyze the outcomes.

Table 3.10. The components of the reaction mix and their stock and final concentrations for the CFPS reaction of the groups contain the pET15b-PS1-N190 with orthogonal Bpa-RS and its corresponding tRNA to produce the PS1 mutant.

Component	Stock concentration	Final concentration\ amount
Master Mix		14.88 µL
Pyruvate kinase	10 mg/mL	0.04 mg/mL
tRNA	40 mg/mL	0.5 mg/mL
T7 RNA polymerase	20 U/mL	0.5 U/mL
Protein inhibitor	100 X	1 X
pET15b-PS1-N190X		1 µg
E. coli lysate	1 X	0.35 X
Bpa-RS		2.15 mg/mL
pBpa	50 mM	0.5 mM
HCl	50 mM	0.5 mM
$tRNA^{opt}_{CUA}$		19649.1 µg\ µL

9. Urea Polyacrylamide Gel Electrophoresis (Urea-PAGE)

Urea-PAGE was performed on a 6% acrylamide gel suitable for separating tRNA sizes between 60 and 75 base pairs (bp) (Albright, n.d.). The total volume of the prepared gel was 60 mL, using the following components: 28.8 g of urea (ultrapure), 13.75 mL of boric acid, 10 mL of 0.5 M EDTA, 60 µL of N, N, N′, N′-Tetramethylethylenediamine (TEMED), 0.6

mL of 10% ammonium persulfate, and 2.4 µl of Gel Red. For sample preparation, 6x loading buffer was used, and samples were heated for 2 minutes at 95°C. A 100-bp DNA marker was used as a reference. The gel was run at 100 volts for 30 minutes (Albright, n.d.).

10. Induction and Expression of Bpa-RS

To enable the expression of Bpa-RS, the same type of media was used to prepare the pre- and main cultures, the Traffic Broth (TB) medium. A 1L of TB was composed of 10 g/L Tryptone, 24 g/L yeast extract, 4 mL glycerol, and 900 mL water. Before use, 100 mL of potassium phosphate buffers (KPI) (0.72, 0.17) M were added to the autoclaved medium.

Table 3.11. The components of the reaction mix and their stock and final concentrations for the CFPS reaction of the group contain the pET15b-PS1 plasmid with orthogonal Bpa-RS and its corresponding tRNA produce wild PS1 as a positive control.

Component	Stock concentration	Final concentration
Master Mix		14.88 µL
Pyruvate kinase	10 mg/mL	0.04 mg/mL
tRNA	40 mg/mL	0.5 mg/ml
T7 RNA polymerase	20 U/mL	0.5 U/ml
Protein inhibitor	100 X	1 X
pET15b-PS1		1 µg
E. coli lysate	1 X	0.35 X
Bpa-RS		2.15 mg/mL
Bpa	50 mM	0.5 mM
HCl	50 mM	0.5 mM
$tRNA^{opt}_{CUA}$		19649.1 µg\ µL

Pre-culture was initiated by inoculating one or two colonies of BL21γ::DE3 cells carrying the PET2Vb-TEV-Bpa-RS plasmid in 500 mL of TB. This medium was supplemented with 50 mL of each of the two buffers of KPI and 0.5 mL of 50 mg/mL kanamycin. 4L of TB media for the main culture were prepared with the addition of 400 mL of each of the two buffers

(KPI) and 4 mL of kanamycin. The cultivation process was continued until the O.D. at 600 nm became 0.5 at 37 °C with agitation at 150 rpm. Protein induction was then started.

Table 3.12. The components of the reaction mix and their stock and final concentrations for the CFPS reaction of the group contain the pET15b-PS1 plasmid without orthogonal Bpa-RS and its corresponding tRNA as the control group to produce mutant PS1.

Component	Stock concentration	Final concentration
Master Mix		14.88 µL
Pyruvate kinase	10 mg/mL	0.04 mg/mL
tRNA	40 mg/mL	0.5 mg/mL
T7 RNA polymerase	20 U/mL	0.5 U/mL
Protein inhibitor	100 X	1 X
pET15b-PS1		1 µg
E. coli lysate	1 X	0.35 X
Bpa-RS		0
Bpa	50 mM	0.5 mM
HCl	50 mM	0.5 mM
$tRNA^{opt}_{CUA}$		0

The induction process for expression of Bpa-RS was initiated after adding a 1:1000 dilution of 1 mM isopropyl-β-D-1-thiogalactopyranoside (IPTG) (K. Ozawa & C. T. Loh, 2014). The process continued for 4 hours at 28°C with shaking at 200 rpm. Following that, the cells are collected by centrifugation at 5000 xg for 30 minutes at 4°C and stored at -80°C.

Table 3.13. The components of feeding mix buffer and their stock and final concentrations for the CFPS system in the optimization of plasmid amount experiment.

Component	Stock concentration	Final concentration
Tris-acetate, pH 8.2	1 M	10 mM
Magnesium acetate	1 M	14 mM
Potassium acetate	10 M	60 mM
DTT	1 M	0.5 mM
H2O		1744.2µL

11. Induction and Expression of TEV Protease

Pre-and main cultures were prepared with 25 g of LB broth powder per 1 L. After the transformation, a pre-culture was prepared by selecting one or more colonies of BL21 DE3 RIL E. coli that grow successfully on an agar plate with ampicillin and chloramphenicol. These colonies were inoculated with 1:1000 dilutions of 200 mg/mL ampicillin and 30 mg/mL chloramphenicol in 100 mL of LB media.

Table 3.14. The components of feeding mix buffer and their stock and final concentrations for the CFPS system in the optimization of plasmid amount experiment.

Component	Stock concentration	Final concentration
Master Mix		1428.63 µL
Feeding mix buffer	1 X	0.35 X
Amino acid mix	40 mg/mL	0.5 mg/mL
H2O		531.79 µL

10 mL of pre-culture were used to inoculate 1L of LB with the appropriate antibiotics for the main culture. The cells were cultivated at 37°C under shaking at 180 rpm. When the O.D. at 600 nm of cells reached 0.6-0.8, they were transferred to the cold room for 15 minutes. 1 mM IPTG was then added to the cultivated cells, and they were incubated for 4 h at 30°C. The cells were then harvested by centrifugation at 6000–9000 rpm for 30 minutes and stored at -80°C.

12. TEV protease activity

To confirm that the purified TEV protease could cleave the His tag of the Bpa-RS protein, small-scale experiments were carried out. A constant amount of the Bpa-RS with varying amounts of TEV protease was present in each 200 µl sample in volume ratios of 1:1, 1:2, 1:3, 1:4, 1:5, 1:0, and 0:1 (Bpa-RS to TEV protease) (**Table 3.5**). Each sample was supplemented with water (**Table 3.5**), and the reaction buffer was composed of 50 mM Tris-base, 25 mM NaCL, 10% glycerol, 2 mM DDT, and 0.5 mM EDTA at pH 8 (**Table 3.5**). The activity tests

were carried out in small tubes overnight at room temperature with shaking. The results were analyzed by SDS-PAGE, followed by western blotting analysis.

Table 3.15. The components of the master mix and their stock and final concentrations for the CFPS system in the optimization of plasmid amount experiment.

Component	Stock concentration	Final concentration
6 Amino acid mix	16.7 mM	1 mM
Amino acid mix	25 mM	0.5 mM
Li,K ACP	1 M	20 mM
PEP	1 M	20 mM
75X NTP mix	90 mM ATP; 60 mM G/C/UTP	1.2 mM ATP; 0.8 mM G/C/UTP
DTT	500 mM	2 mM
Folinic acid (Ca2+)	10 mg/mL	0.1 mg/mL
Complete protease inhibitor	100 X	1 X
HEPEA/EDTA buffer	24 X	1 X
Magnesium acetate	1 M	16 mM
Potassium acetate	4 M	270 mM
PEG 8000	40% (w/v)	2% (w/v)
Sodium azide	10% (w/v)	0.05% (w/v)
H2O		54.4µL

13. Opening cells

Opening cells was a critical step in proceeding with the purification of TEV protease and Bpa-RS. This procedure was performed in both experiments identically, except for the alterations in the lysis buffer used

Table 3.16. The components of the reaction mix and their stock and final concentrations for the CFPS system in the optimization of the plasmid amount experiment for Group 1.

Component	Stock concentration	Final concentration\amount
Master Mix		14.88 µL
Pyruvate kinase	10 mg/mL	0.04 mg/mL
tRNA	40 mg/mL	0.5 mg/mL
T7 RNA polymerase	20 U/mL	0.5 U/mL
Protein inhibitor	100 X	1 X
Plasmid (GFP-PS1)		0
E. coli lysate	1 X	0.35 X
H2O		15.45

Table 3.17. The components of the reaction mix and their stock and final concentrations for the CFPS system in the optimization of the plasmid amount experiment for Group 2.

Component	Stock concentration	Final concentration\amount
Master Mix		14.88 µL
Pyruvate kinase	10 mg/mL	0.04 mg/mL
tRNA	40 mg/mL	0.5 mg/mL
T7 RNA polymerase	20 U/ml	0.5 U/ml
Protein inhibitor	100 X	1 X
Plasmid (GFP-PS1)		0.6 µg
E. coli lysate	1 X	0.35 X
H2O		12.345

Cells were suspended in a lysis buffer tenfold greater than the cell volume, in addition to 0.1 mg/g of cells of DNase, 10 mg/g of Lysosome, and an inhibitor cocktail that includes E64, Pepstain A, Leupeptin, AEBF AEBSF hydrochloride, PMSF, and Benzamine at the working concentration listed in **Table 3.6**. Opening cells were performed using an Emulsi Flex-C (Boulder, 2018), followed by centrifugation at 1000 rpm for 30 minutes at 4°C.

14. Ni-Indigo purification for TEV protease

Ni-Indigo purification for TEV protease was performed using specific prepared buffers. Lysis buffer is composed of 20 mM Tris base, 0.5 M NaCl, 10% glycerol, 100 mM imidazole, and a pH of 8 with a total volume of 200 ml.

Table 3.18. The components of the reaction mix and their stock and final concentrations for the CFPS system in the optimization of the plasmid amount experiment for Group 3.

Component	Stock concentration	Final concentration\ amount
Master Mix		14.88 µL
Pyruvate kinase	10 mg/mL	0.04 mg/mL
tRNA	40 mg/mL	0.5 mg/mL
T7 RNA polymerase	20 U/mL	0.5 U/ml
Protein inhibitor	100 X	1 X
Plasmid (GFP-PS1)		0.8 µg
E. coli lysate	1 X	0.35 X
H2O		11.445

Moreover, the purification process employed two other buffers: ETI-EVI was composed of 20 mM Tris base, 0.5 M NaCl, 10% glycerol, and 300 mM imidazole at a pH of 8 with a volume of 200 mL, and EVII was composed of 20 mM Tris base, 0.5 M NaCl, 10% glycerol, 750 mM imidazole at a pH of 8 with a volume of 50 mL. The bed volume was 20 mL of Ni-Indigo agarose.

The method used to purify TEV protease was as follows: Initially, the purification system was rinsed with water and lysis buffer. The lysed cell solution was then mixed with the beads and incubated on a shaker for 4 h at 4°C. After the incubation, the bead suspension was loaded onto a column and allowed to drain by gravity.

Table 3.19. The components of the reaction mix and their stock and final concentrations for the CFPS system in the optimization of the plasmid amount experiment for Group 4.

Component	Stock concentration	Final concentration\ amount
Master Mix		14.88 µL
Pyruvate kinase	10 mg/mL	0.04 mg/mL
tRNA	40 mg/mL	0.5 mg/mL
T7 RNA polymerase	20 U/mL	0.5 U/mL
Protein inhibitor	100 X	1 X
Plasmid (GFP-PS1)		1 µg
E. coli lysate	1 X	0.35X
H2O		10.625

ETI-EVI buffer was added to the column and followed by EVII buffer, which was used to elute the TEV protease. The concentration of the elution sample was determined using a nanodrop device (A260/A280 ratio), and the presence of protein in the elution sample was visualized by SDS-PAGE with western blot analysis.

15. Ni-Indigo purification of Bpa-synthetase

Ni-Indigo purification of Bpa-RS, both with and without the His tag, follows the same steps and is similar to Ni-Indigo purification for TEV protease but differs in the buffers. Lysis buffer includes 50 mM HEPES, 300 mM NaCl, 5% (w/v) glycerol, 10 mM imidazole, and a pH of 7 with a total volume of 200 ml. The washing buffer contains 50 mM HEPES, 300 mM NaCl, 5% (w/v) glycerol, and 20 mM imidazole at a pH of 7 with a volume of 200 ml. The elution buffer consists of 50 mM HEPES, 300 mM NaCl, 5% (w/v) glycerol, and 500 mM imidazole at a pH of 7, with a volume of 50 ml. The bed volume is 20 mL of Ni-Indigo agarose (K. Ozawa & C. T. Loh, 2014).

Table 3.20. The components of the reaction mix and their stock and final concentrations for the CFPS system in the optimization of the plasmid amount experiment for Group 5.

Component	Stock concentration	Final concentration\ amount
Master Mix		
Pyruvate kinase	10 mg/mL	0.04 mg/mL
tRNA	40 mg/mL	0.5 mg/mL
T7 RNA polymerase	20 U/mL	0.5 U/ml
Protein inhibitor	100 X	1 X
Plasmid (GFP-PS1)		1.2 µg
E. coli lysate	1 X	0.35 X
H2O		9.635

16. Cleavage reaction

According to the activity test, the dialysis bag had a 1:2 volume ratio of Bpa-RS to TEV protease that was then immersed in a buffer solution composed of 50 mM Tris base, 25 mM NaCl, 10% glycerol, 2 mM DDT, and 0.5 mM EDTA at a pH of 8. After that, the mixture was incubated at room temperature overnight with shaking.

Table 3.21. The components of the reaction mix and their stock and final concentrations for the CFPS system in the optimization of the plasmid amount experiment for Group 6.

Component	Stock concentration	Final concentration\ amount
Master Mix		14.88 µL
Pyruvate kinase	10 mg/mL	0.04 mg/mL
tRNA	40 mg/mL	0.5 mg/mL
T7 RNA polymerase	20 U/mL	0.5 U/ml
Protein inhibitor	100 X	1 X
Plasmid (GFP-PS1)		1.5 µg
E. coli lysate	1 X	0.35 X
H2O		8.285 µL

17. Dialysis of Protein

Dialysis buffer (50 mM Tris HCl (PH = 8), 25 mM NaCL, 10% Glycerin, 2 mM Dithiothreitol, 0.5 mM EDTA), pre-treatment buffer (2% (w/v) $NaHCO_3$, 1 mM EDTA), and storage buffer (50% ethanol, 1 mM EDTA) were prepared. 50 mL of protein after the purification process (Bpa-RS/TEV protease) was added to the dialysis bag. Then, the filled dialysis bag was placed in 1 L of dialysis buffer. The dialysis buffer was changed every 2-3 hours for 2-3 times at 4°C.

The dialysis bag was immersed in pre-treatment buffer and then boiled for 10 minutes. It was followed by immersing in water and boiling for 10 minutes, then stored for further experiments by submerging it in the storage buffer at 4°C. The treated bags before use were submerged in H_2O and then in the dialysis buffer. The samples containing the protein were pipetted into the bag and left at 4°C overnight with shaking.

	Volume (ml) of Components Required to Cast Gels of Indicated Volumes							
Components **Gel Volume⇨**	**1 ml**	**2 ml**	**3 ml**	**4 ml**	**5 ml**	**6 ml**	**8 ml**	**10 ml**
H_2O	0.68	1.4	2.1	2.7	3.4	4.1	5.5	6.8
30% acrylamide mix	0.17	0.33	0.5	0.67	0.83	1.0	1.3	1.7
Tris-Cl (1.0 M, pH 6.8)	0.13	0.25	0.38	0.5	0.63	0.75	1.0	1.25
SDS (10%)	0.01	0.02	0.03	0.04	0.05	0.06	0.08	0.1
ammonium persulfate (10%)	0.01	0.02	0.03	0.04	0.05	0.06	0.08	0.1
TEMED	0.001	0.002	0.003	0.004	0.005	0.006	0.008	0.01

Figure 3.1. The components and their volume needed to prepare a 5% staking gel for tris-glycine SDS-PAGE

18. Cell-free protein expression reaction in a continuous exchange (Dialysis)

For the in vitro protein expression experiment, three set-ups were tested: The pET15b-PS1 plasmid with orthogonal Bpa-RS and its corresponding tRNA, the pET15b-PS1-N190 with orthogonal Bpa-RS and its corresponding tRNA, and the control group.

The protocol described in (Kiyoshi Ozawa & Choy Theng Loh, 2014) was being followed for cell-free protein expression reaction in a continuous exchange (dialysis) setting. Moreover, this system was constructed following the cube Biotech protocol of cell-free protein expression reaction in a continuous exchange (dialysis) (Biotech, 2014) (Roos et al., 2014). E. coli S30 was used as part of the CFPS system (Adachi et al., 2019).

Tables 3.7 through 3.12 detail the parameters under that the experiments were conducted. The results were analyzed by western blot after 16 h of reaction and incubation at 30°C and 300 rpm using a shaker-incubator. The cell-free system for protein expression was used at an analytical scale (100 µL) for parameters such as concentration of all components and DNA templet.

	Volume (ml) of Components Required to Cast Gels of Indicated Volumes and Concentrations							
Components **Gel Volume =>**	**5 ml**	**10 ml**	**15 ml**	**20 ml**	**25 ml**	**30 ml**	**40 ml**	**50 ml**
H_2O	1.1	2.3	3.4	4.6	5.7	6.9	9.2	11.5
30% acrylamide mix	2.5	5.0	7.5	10.0	12.5	15.0	20.0	25.0
Tris-Cl (1.5 M, pH 8.8)	1.3	2.5	3.8	5.0	6.3	7.5	10.0	12.5
SDS (10%)	0.05	0.1	0.15	0.2	0.25	0.3	0.4	0.5
10% ammonium persulfate	0.05	0.1	0.15	0.2	0.25	0.3	0.4	0.5
TEMED	0.002	0.004	0.006	0.008	0.01	0.012	0.016	0.02

Figure 3.2. The components and their volume needed to prepare 15% resolving gel for tris-glycine SDS-PAGE

19. Optimization of the amount of Plasmid in CFPS using eGFP

For optimization of the amount of plasmid in CFPS, the pET28a-GfP-PS1 plasmid (221.6 µg/µL) was used. pET28a-GfP-PS1 plasmid was plated on a 1.5% agar plate with a 1 mg/mL Kanamycin antibiotic, expressed in the Top 10 competent cells, and extracted with Plasmid Kit Jel Gene Maxi prep (Scientific, 2024).

According to the protocol for cell-free protein expression reactions in continuous exchange (dialysis) (Biotech, 2014), the plasmid amount should be varied between 0.6 and 1.5 µg in 50 µL tubes. The following amounts were tested to determine the optimal amount of plasmid required for expression: 0, 0.6, 0.8, 1.0, 1.2, and 1.5 µg, respectively.

Tables 3.13, 3.14, and 3.15 display the components of the feeding mix buffer, feeding mix, and master mix for all groups (1-6). **Tables 3.16 through 3.21** show the reaction mix for each of the six groups.

To set up the calibration curve, eGFP was used at a concentration of 1.64 mg/mL. The purification buffer consisted of 50 mM Tris, 200 mM NaCl, and a pH of 7.5. The experiment was done in two parts. For part A (to detect the optimal amount of protein), 10-fold serial dilutions of eGFP at a concentration of 1.64 mg/mL were prepared. The dilutions used were 1.26 mg/mL, 0.126 mg/mL, 0.0126 mg/mL, 0.00126 mg/mL, 0.000126 mg/mL, 0.0000126 mg/mL, and 0.00000126 mg/mL, respectively.

Part B focused on the measurement of the amount of eGFP protein produced by the in vitro system. For this part, 70 µL of eGFP purification buffer were added to 30 µL of each sample (1 through 6) in a 96-well plate. The samples were incubated for 16 h at 300 rpm at 30°C on a shaker-incubator. Post-incubation, a fluorescence plate reader was used to determine the fluorescence of each sample, and the results were plotted on a calibration curve to depict the

relationship between the fluorescence intensity and protein concentration, allowing for precise quantification of the eGFP synthesis in the CFPS system under different conditions.

20. Sodium Dodecyl Sulfate Polyacrylamide Gel Electrophoresis (SDS-PAGE)

Sodium Dodecyl Sulfate Polyacrylamide Gel Electrophoresis (SDS-PAGE) is a technique used to separate proteins according to their molecular weight (BioMart; H. Biotech; Research). In this study, SDS-PAGE was used to analyze Bpa-RS, TEV protease, and mutant PS1, followed by western blot and Coomassi blue staining.

Sample preparation was done by adding 5X loading buffer (500 mM DTT, 10% SDS, 50% glycerol, 0.5% bromophenol blue dye, and 250 mM Tris-HCL, pH= 6.8). The samples were heated to 95°C in a heating block for 10 minutes, then centrifuged for 10 minutes to collect the supernatants.

For gel preparation, 5% stacking gel and 15% resolving gel were prepared and allowed to polymerize for 30 minutes for each. **Figures 3.1 and 3.2** show the solutions for preparing 5% staking gels and 15% resolving gels for tris-glycine SDS-Polyacrylamide Gel electrophoresis.

1x SDS Running buffer was prepared by diluting 10x SDS buffer that consisted of 60.4 g Tris-base, 20 g SDS, and 288 g Glycine to a total volume of 2 L. The prepared running buffer was then poured into the electrophoresis apparatus (Bio-Rad mini protean tetra cell).

The same amount of protein, 30 µg per lane, was loaded into the wells of the SDS-PAGE gel, with one well containing a protein ladder (BLUelf Prestained Protein Ladder) as the molecular weight standard. The gel was then run for 30 minutes at 80 volts until the samples migrated from the staking gel into the resolving gel. Then it was continued to run almost for 1 hour at 120 volts for further separation.

21. Western blot

Western blot analysis was conducted using specific antibodies (Abcam; Bio-Rad; Mahmood & Yang, 2012). His tag antibodies at a 1:1000 dilution were used to detect the protein of interest according to its molecular size.

PVDF membrane was prepared and wetted in methanol for 30 seconds, then soaked with the filter papers in 1x transferring buffer consisting of 39 mM glycine, 48 mM Tris-base, and 20% methanol.

The gel was removed from the SDS-PAGE apparatus, washed with water, and then soaked in 1x transferring buffer. The transfer sandwich was prepared, and semi-dry transferring was done using a blotting apparatus (Trans-Blot Turbo Transfer System). After the transfer, the PVDF membrane was incubated in a blocking solution (0.5% m/v non-fat milk dissolved in T-BST) for 1 hour at room temperature with gentle shaking. Antibodies were then added, and the PVDF membrane was incubated for 2 hours at room temperature with gentle rocking.

After the incubation with antibodies, the PVDF membrane was washed two times with T-BST (10% of 10X TBS, 0.1% of Tween 20) for 20 minutes at room temperature and once with 1X TBS (10X TBS composed of 3M NaCL, 35 mM Tris base, and 165 mM Tris-HCL) for 1 hour at room temperature with gentle shaking.

For the detection, the ECL substrate was prepared just before the detection step. The PVDF membrane was then incubated with ECL substrate for 1 minute. Following this, the Bio-Rad ChemiDoc Imaging System, utilizing Image Lab Touch software, was used to analyze the results.

22. Coomassie Blue Staining

The gel after SDS-PAGE was stained with 10% Coomassi Blue Stain (G-Biosciences; University, n.d.) overnight at room temperature with gentle shaking. Coomassi Blue Stain

(1L) was composed of 118 mL of 85% phosphoric acid, 100 g of ammonium sulfate, and 1.2 g of Coomassie G-250 dissolved in 200 mL of methanol. The volume was then brought to 1L with water. Once the gel is stained, a destaining solution was added to the gel for 4 hours. The destaining solution was prepared by combining 400 mL of methanol with 100 mL of acetic acid and bringing the volume to 1 L with water. A ChemiDoc Imaging System, programmed with Image Lab Touch software, was used to analyze the results.

Chapter Four: Results

This chapter details the results of the experimental procedures and analytical methods employed in this study.

1. Double digestion and electrophoresis of plasmids

In this study, four plasmids were analyzed using double digestion and electrophoresis with the appropriate restriction enzymes, buffers, and conditions specific to each double digestion system (**Tables. 3.2 and 3.3**). A 1 KB ladder was used as a molecular weight marker during electrophoresis to ensure the measurements were accurate and to analyze the results.

1.1. Analysis of pET2b-TEV-Bpa-RS plasmid

For the pET2Vb-TEV-Bpa-RS plasmid that had the fragment of the Bpa-RS gene, I applied the restriction enzymes XhoI and NdeI, both singly and in combination. Surprisingly, when XhoI and NdeI were used independently, no particular band correlating to the Bpa-RS gene was observed.

When the restriction enzymes were combined, the scenario changed, and a distinct band of 921 bp was observed, indicating successful detection of the Bpa-RS gene. The appearance of these bands together with another band of 5327 bp, which refers to the entire plasmid. This confirmed the presence of the Bpa-RS gene within the pET2Vb-TEV-Bpa-RS plasmid **(Fig. 4.1)**.

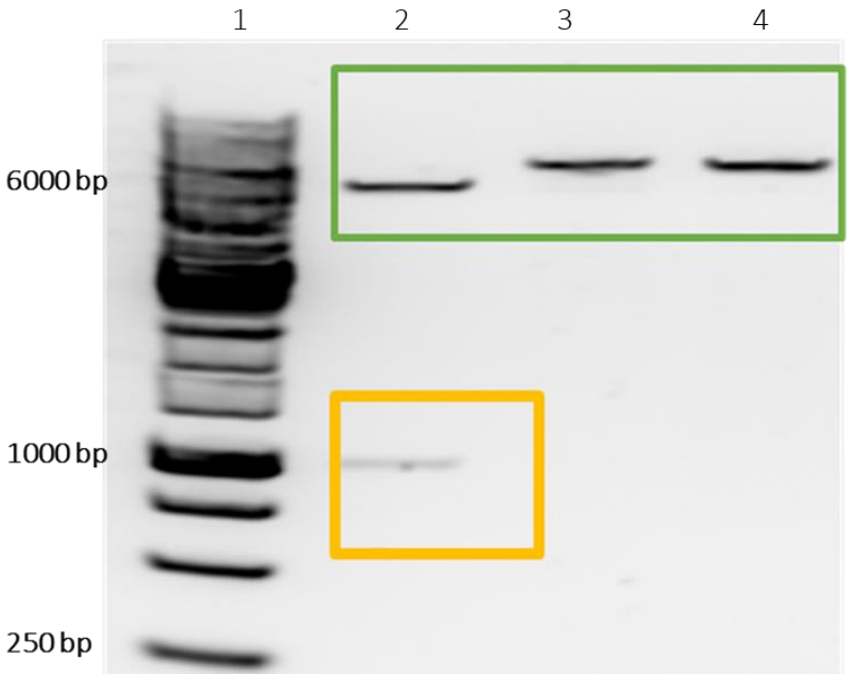

Figure 4.1. Restriction enzyme digestion of the pET2Vb-TEV-Bpa-RS plasmid carrying Bpa-RS gene.

Lane 1: Molecular weight ladder (1 KB ladder). Lane 2: pET2Vb-TEV-Bpa-RS plasmid digested by XhoI and NdeI, showing a band of 921 bp for Bpa-RS. Lane 3: pET2Vb-TEV-Bpa-RS plasmid digested by XhoI. No band was observed. Lane 4: pET2Vb-TEV-Bpa-RS plasmid digested by NdeI. No band was observed. A 5327 bp band was observed in all lanes indicating the intact plasmid. Table 1 details the double digestion process and components. 1% agarose gel electrophoresis was used to confirm the presence of the gene. DNA sample mixed with 6x loading buffer, heated 95°C. Bands were visualized using a Bio-Rad ChemiDoc Imaging System with Image Lab Touch software. Green box: A band of ~6000 bp. Yellow box: A band of ~1000 bp. Size of Bpa-RS: 921 bp.

1.2. Verification of the $tRNA_{CUA}^{opt}$ gene in a pETVOL-$tRNA_{CUA}^{opt}$ plasmid

To confirm the presence of the $tRNA_{CUA}^{opt}$ gene in the pETVOL-$tRNA_{CUA}^{opt}$ plasmid, double digestion was performed using BamH1 and Nco1, both individually and in combination. Electrophoresis results showed that no specific band related to the $tRNA_{CUA}^{opt}$ gene appeared when the digestion was performed with only one enzyme, but a band for the entire plasmid (approximately 3859 bp) was observed. The outcomes of the combined double digestion efficiently demonstrated the presence of the $tRNA_{CUA}^{opt}$ gene within the plasmid, as indicated by an 882 bp band **(Fig. 4.2)**.

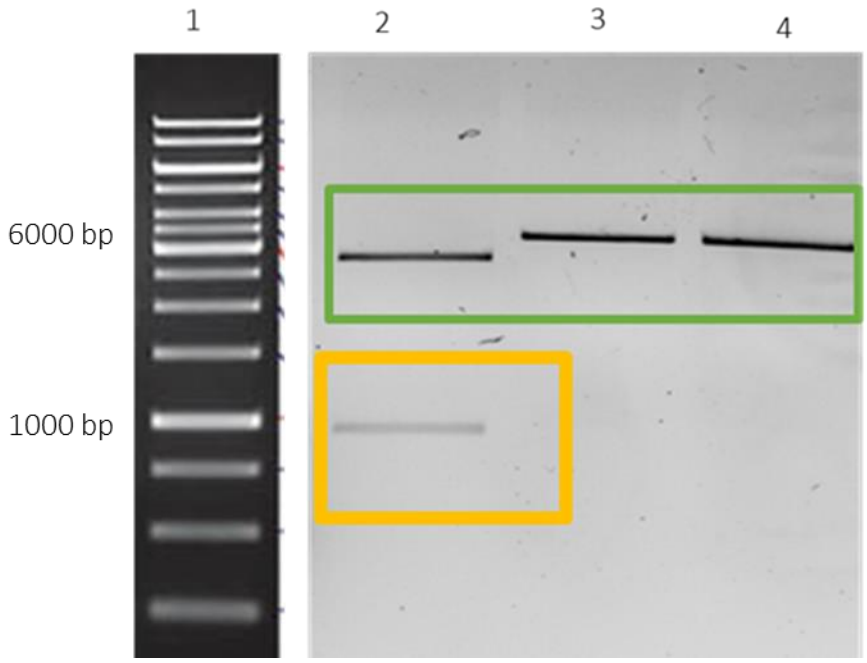

Figure 4.2. Restriction enzyme digestion of the pETVOL-tRNA$_{CUA}^{opt}$ plasmid carrying tRNA$_{CUA}^{opt}$ gene.

Lane 1: pETVOL-tRNA$_{CUA}^{opt}$ plasmid digested by BamH1 and Nco1, showing the correct band of 882 bp for tRNA$_{CUA}^{opt}$. Lane 2 and 3: pETVOL- tRNA$_{CUA}^{opt}$ plasmid digested by BamH1 and Nco1 separately. No specific band was observed in lane 2 and 3. A 5327 bp band was observed in all lanes indicating the intact pETVOL-tRNA$_{CUA}^{opt}$ plasmid. Table 1 details the double digestion process and components. 1% agarose gel electrophoresis was used to confirm the presence of the gene. DNA sample mixed with 6x loading buffer, heated 95°C. Bands were visualized using a Bio-Rad ChemiDoc Imaging System with Image Lab Touch software. Green box: A band of ~6000 bp. Yellow box: A band of ~1000 bp. Size of tRNA$_{CUA}^{opt}$ gene: 882 bp.

1.3.Confirmation of PS1-N190-amber in pET15b-PS1-N190-amber plasmid

Double digestion was conducted by Xhol and Nde1 to confirm the presence of the PS1-N190-amber gene (PS1 mutant gene) within the pET15b-PS1-N190-amber plasmid. The pET15b-PS1 plasmid, which contained the PS1 gene, was used as a reference. The electrophoresis results of the reference showed a faint band at 1401 bp, indicating the presence of the PS1 gene, alongside another band for the whole plasmid (approximately 6000 bp). The outcomes for pET15b-PS1-N190-amber were particularly crucial; the band 1401bp was more obvious and clearer, indicating that the mutated PS1 gene was present in this plasmid **(Fig. 4.3)**.

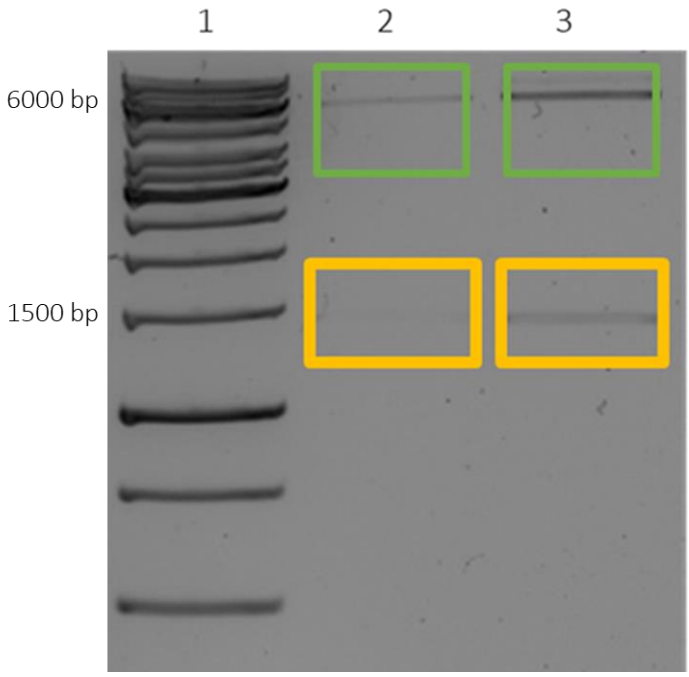

Figure 4.3. Restriction enzyme digestion of pET15b-PS1-N190-amber plasmid contains PS1-N190-amber gene (PS1 mutant gene).

Lane 1: Molecular weight ladder (1 KB ladder). Lane 2: pET15b-PS1 digested by Xhol and Nde1, showing a faint band at 1401 bp for PS1. Lane 3: pET15b-PS1-N190-amber plasmid digested by Xhol and Nde1, a clear band at 1401 bp for the PS1-N190-amber gene was obvious. Approximately 6000 bp bands were observed in lanes 2 and 3 indicating the intact pET15b-PS1-N190-amber plasmid and pET15b-PS1 plasmid. Table 1 details the double digestion process and components. 1% agarose gel electrophoresis was used to confirm the presence of the gene. DNA sample mixed with 6x loading buffer, heated 95°C. Bands were visualized using a Bio-Rad ChemiDoc Imaging System with Image Lab Touch software. Green box: A band of ~6000 bp. Yellow box: A band of ~1500 bp. Size of PS1-N190-amber: 1401 bp.

1.4. Examination of GFP and PS1 genes in the pET28aGFP-PS1 plasmid

The pET28aGFP-PS1, which contained both the GFP and PS1 genes, was analyzed using two double digestion systems. The first digestion used the restriction enzymes NdeI and NcoI to confirm the presence of the GFP gene within the pET28aGFP-PS1 plasmid. A 717 bp band was produced as a result, indicating the presence of the GFP gene. The second digestion system used BamH1 and EcoR1 to identify the PS1 gene within the plasmid. This yielded a band at approximately 1404 was observed, indicating the presence of PS1 in the pET28aGFP-PS1 plasmid **(Fig. 4.4)**.

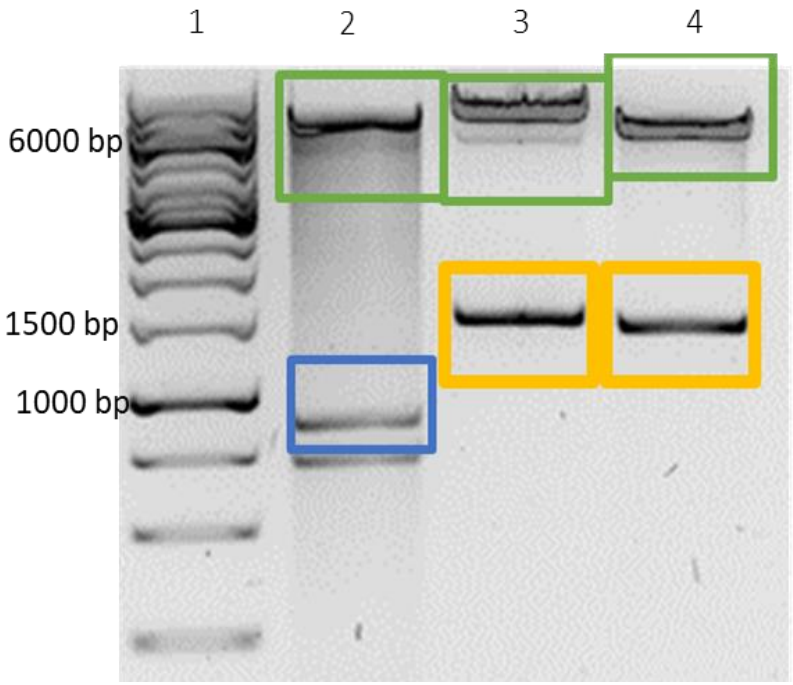

Figure 4.4. Restriction enzyme digestion of pET28aGFP-PS1 plasmid.

Lane 1: Molecular weight ladder (1 KB ladder). Lane 2: pET28aGFP-PS1 digested by Nde1 and Nco1, showing a clear band at 717 bp for GFP. Lane 3: pET28aGFP-PS1 plasmid digested by BamH1 and EcoR1, a clear band at 1404 bp for the PS1 gene was obvious. Lane4: pET15b-PS1 plasmid digested by Xhol and EcoR1, showing an obvious band for the PS1 gene. Approximately 6000 bp bands were observed in lanes 2, 3, and 4 indicating the intact pET28aGFP-PS1 plasmid. Table 1 details the double digestion process and components. 1% agarose gel electrophoresis was used to confirm the presence of the gene. DNA sample mixed with 6x loading buffer, heated 95°C. Bands were visualized using a Bio-Rad ChemiDoc Imaging System with Image Lab Touch software. Green box: A band of ~6000 bp. Yellow box: A band of ~1500 bp. Blue box: : A band of ~1000 bp. Size of GFP gene: 717 bp. Size of PS1 gene : 1404 bp.

A third double digestion with Xhol and EcoR1 was employed on the pET-15bPS1 plasmid to confirm that the 717 bp band belonged to the GFP gene but not the PS1 gene **(Fig. 4.4)**. Distinct bands corresponding to the plasmid sizes (pET28aGFP-PS1 and pET-15bPS1) were observed in each double digestion system **(Fig. 4.4)**.

Establishment and Optimization of an In Vitro Protein Expression System for Full and Functional PS1 Production

An in vitro protein expression system required several steps for set-up and expression of full and functional PS1.

First: Bpa-RS expression and purification

The initial step was to gain the pure Bpa-RS protein through a four-step process as outlined below, ensuring its readiness for downstream experiments.

Step 1: Initial expression and purification of Bpa-RS

The first step was Bpa-RS expression and purification. After the successful expression of the protein in BL21γ::DE3 cells, the initial weight of the cells used was 8 g. IMAC purification was applied with appropriate pH, temperature, and buffers. In addition, dialysis was also performed using a 50 mL volume of liquid, resulting in 23.05 mg of protein. The success of Bpa-RS expression and purification was confirmed by SDS-PAGE, western blot, and staining with Coomassie Brilliant Blue.

The pET2Vb-TEV-Bpa-RS plasmid had a His tag, which helped to indicate Bpa-RS during the purification process through western blot analysis using the appropriate antibodies. A ~35 KD band was observed, matching the expected size of Bpa-RS. Moreover, Coomassie Brilliant Blue staining displayed a band of the same size, confirming that this band was related to the Bpa-RS **(Fig. 4.5)**.

Step 2: Expression and purification of TEV protease

The second step focused on expressing and IMAC purification for the TEV protease. The BL21 DE3 RIL expression system with a pRK93-TEV plasmid was used. The initial weight of the cells used was 13 g.

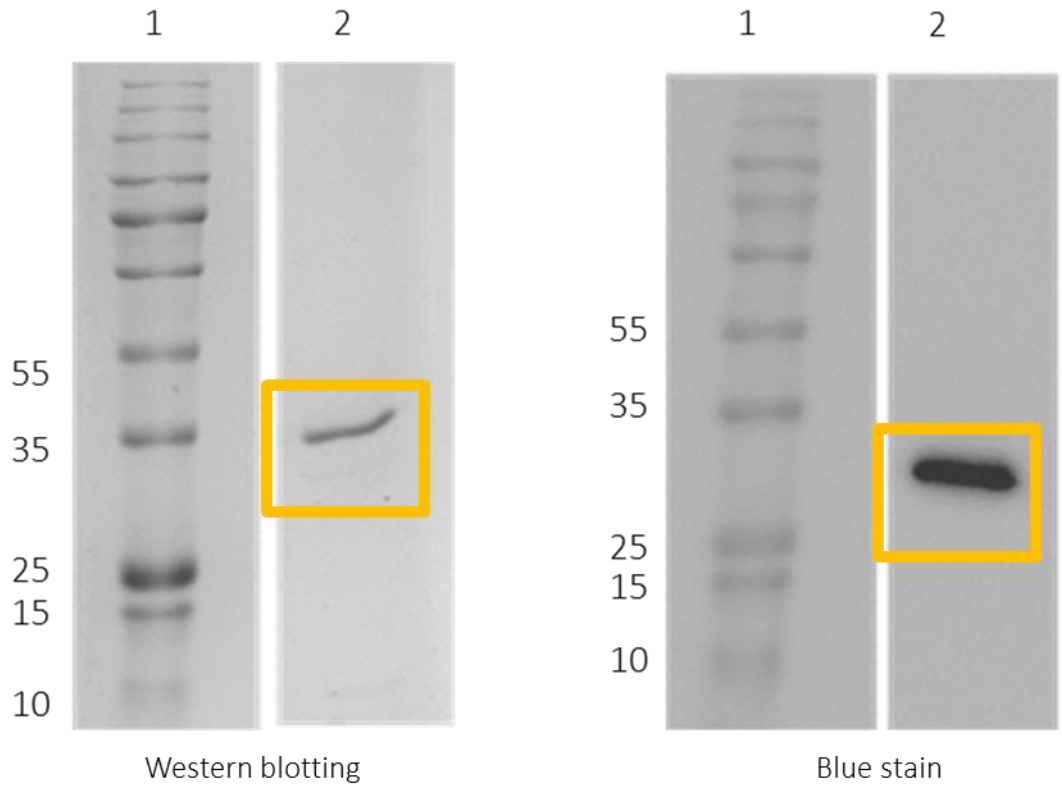

Figure 4.5. Western blot and Coomassie Brilliant Blue staining of IMAC purification of Bpa-RS with His Tag.

Purification of Bpa-RS with His Tag. A. western blot results, indicating the successful purification of Bpa-RS in BL21γ::DE3 with a clear band at ~35 KDa, matching the expected size of Bpa-RS. IMAC purification of Bpa-RS, followed by dialysis, yielded 23.05 mg of protein. Buffers included Lysis buffer includes 50 mM HEPES, 300 mM NaCl, 5% (w/v) Glycerol, 10 mM Imidazole, PH =7. The washing buffer contains 50 mM HEPES, 300 mM NaCl, 5% (w/v) Glycerol, and 20 mM Imidazole, at pH =7. The elution buffer consists of 50 mM HEPES, 300 mM NaCl, 5% (w/v) Glycerol and 500 mM Imidazole at pH =7. Dialysis buffer (50 mM Tris HCl (PH = 8), 25 mM NaCL, 10% Glycerin, 2 mM Dithiothreitol, 0.5 mM EDTA). B. Coomassie Brilliant blue staining results of IMAC purification further confirm the 23.9 KDa band. A ChemiDoc system was used to validate the success of purification of Bpa-RS with His Tag. The Bio-Rad ChemiDoc Imaging System, utilizing Image Lab Touch software, was used to analyze the results. Lane 1: A protein ladder (BLUelf Prestained Protein Ladder). Lane 2: the protein sample. Size of Bpa-synthetase: 34,8KD.

The final yield was 3.55 mg post-dialysis using a 50 mL volume of liquid. SDS-PAGE followed by western blot and staining with Coomassie Brilliant Blue confirmed the successful expression and isolation, with clear bands in both techniques. A 26.8 KD band, corresponding to the expected size of the TEV protease protein, was observed **(Fig. 4.6)**.

Step 3: Determining the effective ratio of Bpa-RS to TEV protease

In the third step, the ideal ratio of the effective activity of TEV protease was determined to proceed with the downstream processing and study of Bpa-RS protein to be ready for use in the CFPS system.

This involved testing several volume ratios of Bpa-RS to TEV protease (1:1, 1:2, 1:3, 1:4, 1:5, 1:0, and 0:1) (Table 3.4). The Bpa-RS volume was consistent at 3 μL and 0.747 mg of protein. To analyze the outcomes, western blot and specific antibodies were used to detect the effective ratio for His-tag-cleaved Bpa-RS. For all tests volume ratios, a visible band corresponding to the size of the TEV protease protein and no bands for the Bpa-RS protein was observed, indicating the loss of the His tag (Fig. 4.7).

Step 4: Large-scale application of Bpa-RS and TEV protease

The fourth step involved scaling up the use of the chosen volume ratio of Bpa-RS and TEV application, attempting to remove His Tag from a larger amount of Bpa-RS, which was planned to be used in the CFPS system.

The volume of Bpa-RS was 15 to 30 mL of TEV protease. The yield amount of Bpa-RS with cleaved His Tag was 1.82 mg using a 45 mL volume of liquid (Bpa-RS and TEV protease). Western blotting was also applied to ensure the removal of the His tag from Bpa-RS. The outcomes showed successful cleavage, as there were no bands related to His-tagged Bpa-RS protein **(Fig. 4.8)**.

Second: Isolation of tRNA

The CFPS system for the synthesis of PS1 is also required to express and isolate tRNA. The expression of tRNA was done using the pETVOL-tRNACUAopt plasmid with the BL21 Star™ (DE3) expression host.

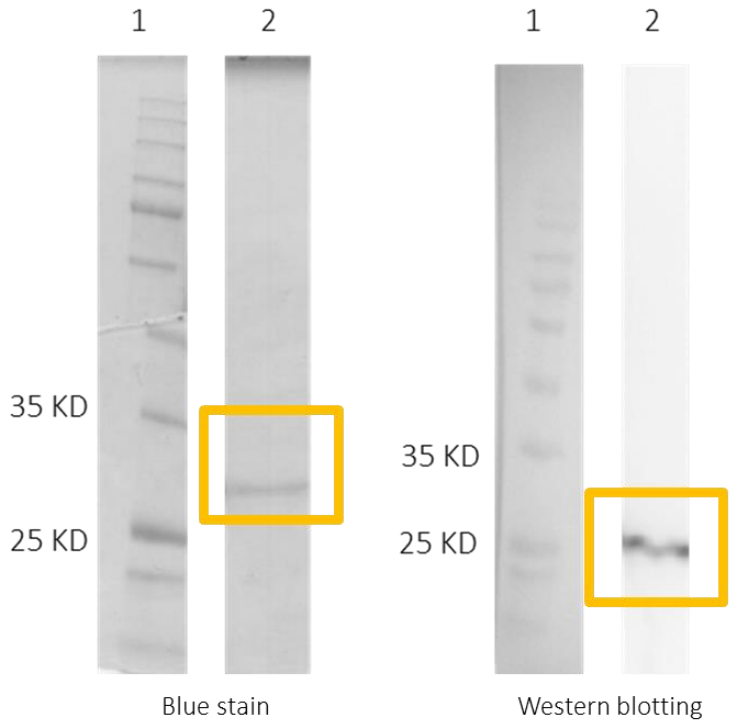

Figure 4.6. Western blot and Coomassie Brilliant Blue staining of IMAC purification of TEV protease protein.

Purification of TEV protease protein. A. western blot results, indicating the successful purification of TEV protease protein in BL21 DE3 RIL with a 26.8 KDa band, corresponding to the expected size of the TEV protease protein, was observed. IMAC purification of TEV protease protein, followed by dialysis. The final yield was 3.55 mg post-dialysis using a 50 mL volume of liquid. The purification process employed two other buffers: ETI-EVI (20 mM Tris base, 0.5 M NaCl, 10% Glycerol, Imidazole 300 mM, pH = 8) and EVII (20 mM Tris base, 0.5 M NaCl, 10% Glycerol, Imidazole 750 mM, pH = 8). Dialysis buffer (50 mM Tris HCl (PH = 8), 25 mM NaCL, 10% Glycerin, 2 mM Dithiothreitol, 0.5 mM EDTA). B. Coomassie Brilliant blue staining results of IMAC purification further confirm the 26.8 KDa band. A ChemiDoc system was used to validate the success of the purification of the TEV protease protein. The Bio-Rad ChemiDoc Imaging System, utilizing Image Lab Touch software, was used to analyze the results. Lane 1: A protein ladder (BLUelf Prestained Protein Ladder). Lane 2: the protein sample. Size of TEV protease: 26,8KD.

Following the protocol of the Phenol-Chloroform extraction for tRNA method that was described in the method, 196.491 µg was obtained. The initial weight of BL21 Star™ (DE3) E. coli cells used was 5.3014 g. The extracted tRNA was subjected to analysis using Urea PAGE, GelRed® Nucleic Acid Gel Stain, and a 100-bp DNA ladder. The result confirmed that the isolation of tRNA was successful, as indicated by a clear band at approximately 70 bp (Fig. 4.9.A).

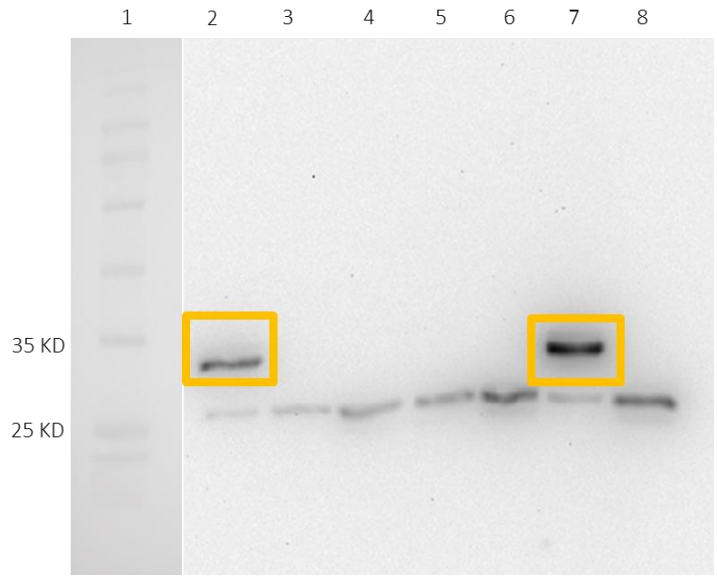

Figure 4.7. Western blot of TEV protease protein activity.

TEV protease protein activity test; various volume ratios of Bpa-RS and TEV protease (1:1, 1:2, 1:3, 1:4, 1:5, 1:0, and 0:1) with a constant amount of Bpa-RS of 0.747 mg are tested. The samples were incubated in a reaction buffer (50 mM Tris-base, 25 mM NaCl, 10% glycerol, 2 mM DTT, 0.5 mM EDTA, pH 8) overnight at room temperature. The effective volume ratio of Bpa-RS and TEV protease was detected by western blot. The 1:2 volume ratio was identified as the first effective combination. A clear band for TEV protease was showen and no band for Bpa-RS. Buffer solution of the cleavage reaction was composed of 50 mM Tris base, 25 mM NaCl, 10% glycerol, 2 mM DDT, and 0.5 mM EDTA, pH = 8. After that, the mixture was incubated at room temperature overnight with shaking. The Bio-Rad ChemiDoc Imaging System, utilizing Image Lab Touch software, was used to analyze the results. Lane 1: A protein ladder (BLUelf Prestained Protein Ladder). Lane 2: The sample of 1:1 ratio. Lane 3: The sample of 1:2 ratios. Lane 4: The sample of 1:3 ratios. Lane 5: The sample of 1:4 ratios. Lane 6: The sample of 1:5 ratios. Lane 7: The sample of 1:0 ratio. Lane 8: The sample of 0:1 ratio. Table 3.4. shows the ratios of Bpa-RS to TEV protease, amounts of Bpa-RS, and TEV protease amounts that were used in the experiment of TEV protease protein activity. Yellow Box: BPA-synthetase. Size of BPA-synthetase: 34,8KD. Size of TEV protease: 26,8KD

To ensure that the protocols of tRNA expression and isolation were efficient, the same protocols were applied in a second attempt to extract tRNA, and the yield of tRNA was 101.2 µg. Then, agarose gel electrophoresis was used to analyze the efficiency of the extraction method. The outcome was an obvious band with a size of 70 pb, corresponding to tRNA. The result of the second extraction is identical to the first extraction **(Fig. 4.9.B)**.

Third: Optimization of the plasmid amount for in vitro protein expression

To determine the ideal amount of plasmid for efficient protein expression, various amounts of pET28a-GFP-PS1 were tested (0, 0.6, 1, 1.2, and 1.5 μg). A fluorescent reader and the calibration curve of eGFP were used to determine the concentration of protein. The results showed that the fluorescence vs. concentration curve for different amounts of the pET28a-GFP-PS1 plasmid exhibited a direct relationship between the amount and the concentration; as the amount increased, the concentration increased as well **(Fig. 4.10)**.

Forth: CFPS system

After 18 hours of incubation at 30°C, and following the protocols (see the methods section), results were analyzed by western blot. The results were not as expected; a truncated protein version was produced in all groups of the experiment, regardless of whether the pET15b-PS1-N190 or pET15b-PS1 plasmid was used or if the orthogonal Bpa-RS and its corresponding tRNA were added. The three distinct 23.9 KD bands were clearly presented **(Fig. 4.11)**.

Chapter Five: Discussion

In this section, the outcomes of this experimental approach will be discussed, which is to creating an effective CFPS system for the synthesis of PS1. PS1 is an important subunit of protein that is associated with the development of AD.

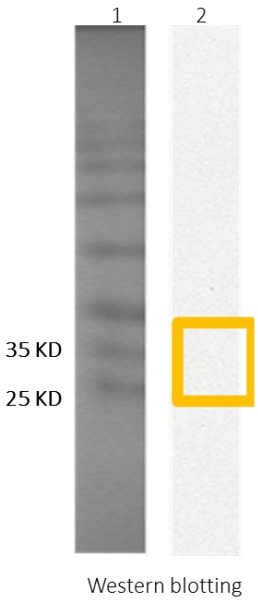

Figure 4.8. Western blot result for IMAC purification of Bpa-RS after His tag cleavage.

The reaction system was established as described in the methods, followed by Ni-Indigo IMAC purification and dialysis. According to the activity test, the dialysis bag had a 1:2 volume ratio of Bpa-RS to TEV protease that was then immersed in a buffer solution composed of 50 mM Tris base, 25 mM NaCl, 10% glycerol, 2 mM DDT, and 0.5 mM EDTA, pH = 8. After that, the mixture was incubated at room temperature overnight with shaking. Ni-Indigo purification was performed using specific prepared buffers. Lysis buffer was composed of 20 mM Tris base, 0.5 M NaCl, 10% Glycerol, Imidazole 100 mM, and pH = 8. Moreover, the purification process employed two other buffers: ETI-EVI (20 mM Tris base, 0.5 M NaCl, 10% Glycerol, Imidazole 300 mM, pH = 8) and EVII (20 mM Tris base, 0.5 M NaCl, 10% Glycerol, Imidazole 750 mM, pH = 8). Dialysis buffer (50 mM Tris HCl (PH = 8), 25 mM NaCL, 10% Glycerin, 2 mM Dithiothreitol, 0.5 mM EDTA). The amount of Bpa-RS was 2.305 mg to 4.61 mg of TEV protease. The yield amount of Bpa-RS with cleaved His Tag was 1.82 mg using a 45 mL volume of liquid (Bpa-RS and TEV protease). Western blotting was also applied to ensure the removal of the tag from Bpa-RS. The outcomes showed successful cleavage, as there were no bands related to the Bpa-RS protein, as the results of western blot analysis showed. This indicated that the cleavage process was successfully completed, and Bpa-RS no longer had its tag. The Bio-Rad ChemiDoc Imaging System, utilizing Image Lab Touch software, was used to analyze the results. Lane 1: A protein ladder (BLUelf Prestained Protein Ladder). Lane 2: a sample of 1:2 volume ratio of Bpa-RS to TEV protease after The reaction system, Ni-Indigo IMAC purification and dialysis. Yellow Box: Bpa-RS with cleaved His Tag. Size of Bpa-synthetase: 34,8 KD.

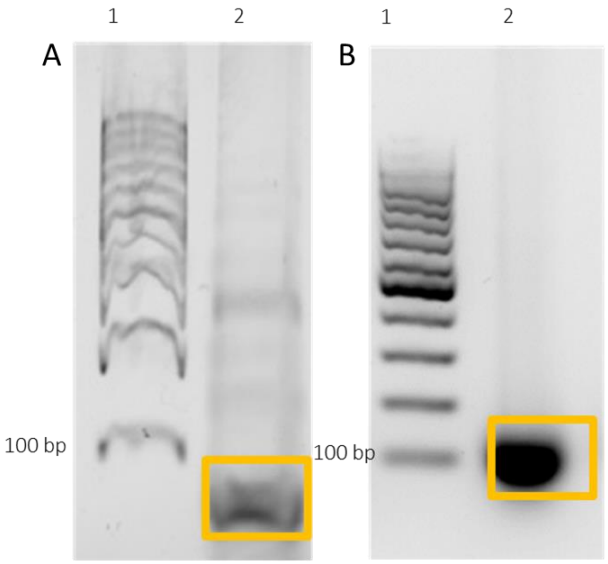

Figure 4.9. Polyacrylamide Gel Electrophoresis (Urea PAGE) and Agarose Gel Electrophoresis of Isolation of tRNA.

A. Polyacrylamide Gel Electrophoresis (Urea PAGE) results of Isolation of tRNA. B. Agarose Gel Electrophoresis of Isolation of tRNA. Using the pETVOL-tRNA plasmid and the BL21 Star™ (DE3) E. coli as host, the tRNA was expressed and extracted using the Phenol-Chloroform extraction protocol. The yield was 196.491 µg. The initial cell mass of 5.3014 g. Polyacrylamide Gel Electrophoresis (Urea PAGE) was used to detect the tRNA, showing a clear band at approximately 70 bp. tRNA size is approximately 70 bp ; this confirmed the successful isolation of tRNA. A second extraction of tRNA was performed using the same extraction method, but agarose gel electrophoresis was used instead to detecte tRNA. Its outcome is identical to the first extraction. This indicated that the extracted tRNA is pure and usable for further molecular experiments. The ratio of A260/A280 at wavelength 260 nm was used to determine the purity of RNA and the protein via a nanodrop device. The Bio-Rad ChemiDoc Imaging System, which was operated with Image Lab Touch software, was used to visualize the tRNA bands. Lane 1: Molecular weight ladder (1 KB ladder). Lane 2: tRNA sample. Yellow box: tRNA.

This study involved a meticulously planned series of experiments focused on plasmid analysis, protein purification, tRNA isolation, and the creation and optimization of CFPS. The main objective was to successfully express the target full-fold functional PS1 and incorporated a specific mutation introduced by genetic engineering techniques.

This experimental approach involved the examination of extracted-plasmids harboring target genes, including Bpa-RS, tRNACUAopt, eGFP, and PS1-N190-amber. This analysis was

performed using double digestion and electrophoresis techniques. After that, Bpa-RS was expressed and purified. IMAC purification and TEV protease-mediated tag cleavage were applied to obtain tag-free Bpa-RS, which is suitable for downstream experiments.

Furthermore, this research project focused on isolating tRNA to bolster the functionality of the CFPS system and then adjusted the plasmid amounts to optimize the efficiency of protein expression. Ultimately, to test the CFPS system's capacity to produce full-length and functional mutant PS1, its performance was examined via western blot analysis on PS1 variants.

1. Analysis of Double Digestion of Plasmid Results

Through this discussion, the study aims to clarify the significance of the outcomes of each experimental step and suggest potential directions for further optimization and developments to enhance the CFPS system's performance for PS1 protein expression. In this study, double digestion and electrophoresis were used to examine a cohort of plasmids, which are essential for establishing the CFPS system. Using this method allowed me to confirm that the plasmid carried the target genes and that they were suitable for the downstream experiments.

1.1. pET2Vb-TEV-Bpa-RS Plasmid

The Bpa-RS gene was not detected by a specific band produced from individual double digestion using XhoI and NdeI enzymes. Nevertheless, successful detection of the Bpa-RS gene was confirmed by a clear band consisting of 921 bp when these enzymes were used in conjugation **(Fig. 4.1)**. This band, along with the band that represents the full plasmid, confirmed the presence of the Bpa-RS gene in the pET2Vb-TEV-Bpa-RS plasmid, indicating that the pET2Vb-TEV-Bpa-RS plasmid is appropriate for further protein studies.

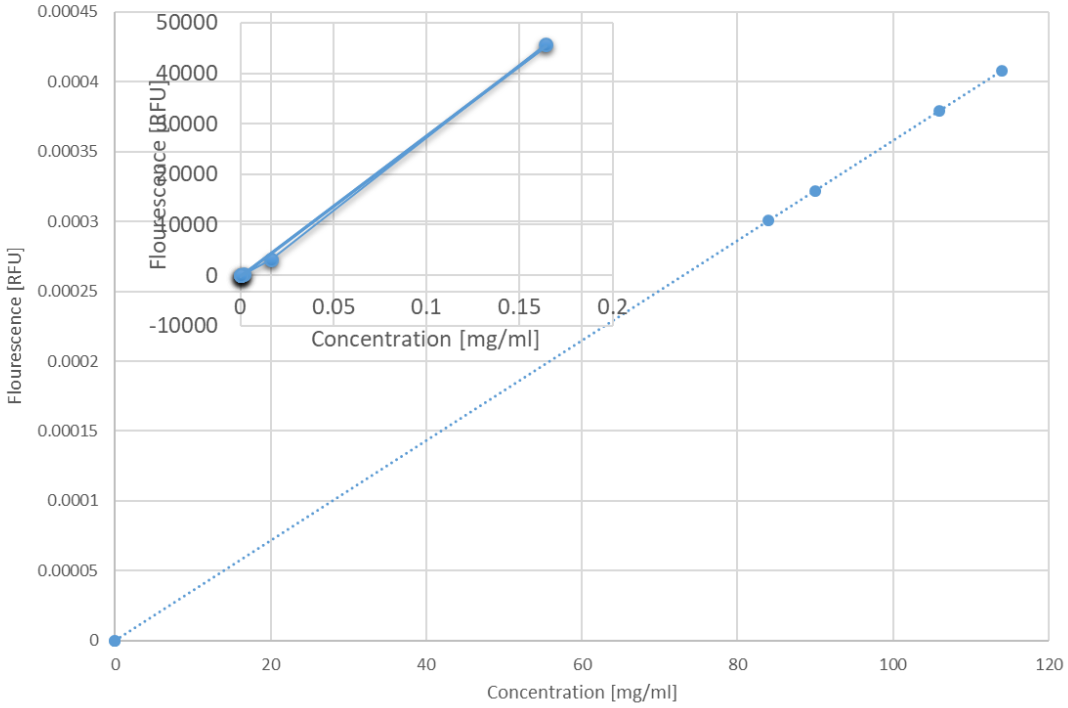

Figure 4.10. Optimization of the Plasmid amount for in vitro protein expression.

Various amounts of pET28a-GFP-PS1 were tested (0, 0.6, 1, 1.2, 1.5 µg) to determine the ideal amount of plasmid for efficient protein expression. A fluorescent reader and the calibration curve of eGFP were used to determine the concentration of protein. The results showed that the fluorescence vs. concentration curve for different amounts of the pET28a-GFP-PS1 plasmid exhibited a direct relationship between the amount and the concentration; as the amount increased the concentration increased as well. Based on this, any tested amount of plasmid could be used in further experiments. To set up the calibration curve, eGFP was used with a concentration of 1.64 mg/mL. The purification buffer consisted of 50 mM Tris, 200 mM NaCl, pH =7.5. 10-fold serial dilutions of eGFP at a concentration of 1.64 mg/mL were prepared to set up the calibration curve. The dilutions used were 1.26 mg/mL, 0.126 mg/mL, 0.0126 mg/mL, 0.00126 mg/mL, 0.000126 mg/mL, 0.0000126 mg/mL, and 0.00000126 mg/mL, respectively. For the fluorescence vs. concentration curve, the measurements focused on the amounts of eGFP protein produced by the in vitro system. For this part, 70 µL of eGFP purification buffer were added to 30 µL of each sample (1 through 6) in a 96-well plate. The samples were incubated for 16 h, 300 rpm, at 30°C on a shaker-incubator. Post-incubation, a fluorescence plate reader was used to determine the fluorescence of each sample and the results were plotted on a calibration curve to depict the relationship between the fluorescence intensity and protein concentration, allowing for precise quantification of the eGFP synthesis in CFPS under different conditions.

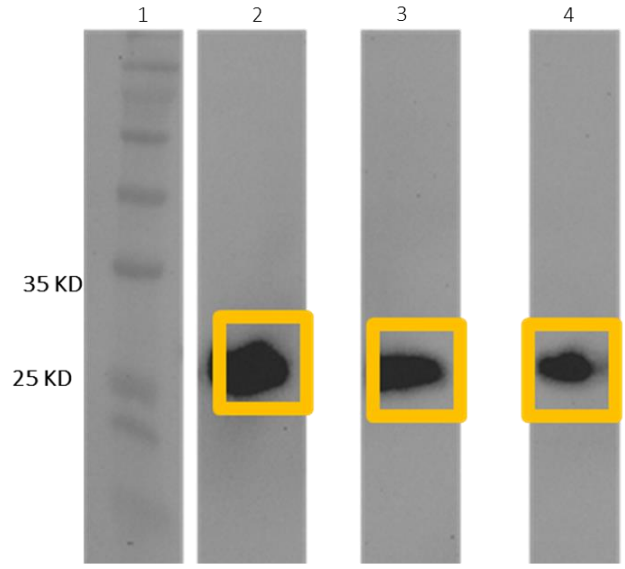

Figure 4.11. Cell-Free Protein Synthesis (CFPS) system.

For the in vitro protein expression experiment, three set-ups were tested: The pET15b-PS1 plasmid with orthogonal Bpa-RS and its corresponding tRNA, the pET15b-PS1-N190 with orthogonal Bpa-RS and its corresponding tRNA, and the control group. The results were analyzed by western blot. After 18 h of incubation at 30°C, and following the protocols (see the methods section). The results were not as expected. The three distinct 23.9 KD bands clearly appeared. A truncated protein version was produced in all groups of the experiment, regardless of whether the pET15b-PS1-N190 or pET15b-PS1 plasmid was used or if the orthogonal Bpa-RS and its corresponding tRNA were added. Lane 1: A protein ladder (BLUelf Prestained Protein Ladder). Lane 2: The sample of protein, which was produced in CFPS system, using the pET15b-PS1 plasmid with orthogonal Bpa-RS and its corresponding tRNA. Lane 3: The sample of protein, which was produced in the CFPS system, using the pET15b-PS1-N190 with orthogonal Bpa-RS and its corresponding tRNA. Lane 4: The sample of protein, which was produced in the CFPS system, using the pET15b-PS1-N190 without orthogonal Bpa-RS and its corresponding tRNA (control group). Yellow box: 23.9 KD bands. Truncated PS1 size: 23.9 KD.

1.2. pETVOL-tRNA Plasmid

The $tRNA_{CUA}^{opt}$ gene was not detected by a specific band after the single digestion with BamHI and NcoI enzymes separately. However, the presence of the $tRNA_{CUA}^{opt}$ gene within the plasmid was confirmed successfully by a band of 882 bp resulting from the combined digestion **(Fig. 4.2)**. This correct detection of the tRNA gene validates the suitability of the pETVOL-tRNA plasmid for assisting the translation process in the CFPS system.

1.3. pET15b-PS1-N190-amber Plasmid

The double digestions with XhoI and NdeI enzymes verified the presence of the PS1-N190-amber gene within the pET15b-PS1-N190-amber plasmid and the PS1 gene's presence within the pET15b-PS1 plasmid. The successful insertion of the target gene was indicated by a 1401 bp band corresponding to the PS1-N190-amber gene, along with a band for the full plasmid at approximately 6000 bp. The same band was produced by the double digestions for the pET15b-PS1 plasmid. This indicated that the PS1-N190-amber gene has the same length as the PS1 gene **(Fig. 4.3)**. This detection ensures the availability of the PS1-N190-amber gene within the pET15b-PS1-N190-amber plasmid for subsequent experiments with the CFPS system.

1.4. pET28aGFP-PS1 Plasmid

The presence of the GFP gene within pET28aGFP-PS1 was confirmed by a 717 bp band corresponding to the GFP gene, using the double digestion technique with NdeI and NcoI enzymes. The next double digestion with BamH1 and EcoR1 produced a band at approximately 1404 bp related to the PS1 gene. This confirmed the presence of PS1 within the pET28aGFP-PS1 plasmid. To verify that the 717 bp band was specific for the GFP gene, a third double digestion system was done with XhoI and EcoR1 on the pET-15bPS1 plasmid as a control lacking the GFP gene. The absence of a 717 bp band in this control indicated that the band seen in pET28aGFP-PS1 is indeed for GFP gene. This result confirms that the pET28aGFP-PS1 plasmid was correctly constructed. The pET-15bPS1 plasmid serves as an appropriate control to distinguish the GFP gene **(Fig. 4.4)**. These outcomes validated that the use of the pET28aGFP-PS1 plasmid was appropriate for further experiments.

The effective application of double digestion and electrophoresis to analyze the plasmids affirmed the presence of the target gene, which is crucial for the CFPS system. This confirmation guarantees the appropriateness and integrity of plasmids for further

experiments, providing a solid basis for the successful expression and synthesis of the desired protein.

2. Expression and purification of Bpa-RS

2.1. Initial expression and purification of Bpa-RS

In this stage of the study, the study aimed to achieve the optimal expression and purification of Bpa-RS, an important protein for subsequent experiments within the CFPS system. The expression process of Bpa-RS involved the use of BL21γ::DE3 cells and the suitable conditions for Bpa-RS induction. After the induction, the protein was purified via IMAC with optimized conditions for temperature, pH, and buffer composition. The purification process yielded 23.05 mg of Bpa-RS, which illustrates effective protein expression and purification. SDS-PAGE followed by western blot was performed to evaluate the purity and molecular weight of the purified Bpa-RS. The efficiency of the purification process was proved by a distinct band after probing with the appropriate antibodies that matched the expected size of Bpa-RS **(Fig. 4.5)**. Moreover, the success of purification was confirmed by Coomassie Brilliant Blue staining of the SDS-PAGE gel, that also showed a clear band at the expected size of Bpa-RS **(Fig. 4.5)**. The two techniques showed close results, enhancing the validity of purification results and confirming that Bpa-RS was pure and could be used in further experiments.

Functional and pure Bpa-RS was required for the CFPS system to produce PS1 variants, serving as an important component in introducing site-specific UAA at the target site. This meant Bpa-RS could be used as an important component to control the synthesis of PS1 variants, thus aiding in the study's progress.

2.2. Tag Cleavage Mediated by TEV Protease

In the preparation of Bpa-RS for further experiments, the cleavage of His-Tag using TEV protease was a crucial step. A series of tests with different conditions were performed to

determine the optimal Bpa-RS to TEV protease volume ratio to cleave His-tag efficiently, ranging from 1:1 to 1:5. Successful cleavage was detected by western blotting with specific antibody probing, which showed bands corresponding to TEV protease at its expected size and the absence of bands for Bpa-RS. The analysis demonstrated that 1:2 was the most effective ratio for tag removal **(Fig. 4.7)**. The downstream application of this study depended on achieving the optimal Bpa-RS to TEV protease volume ratio. Complete cleavage of the His tag ensured that the Bpa-RS protein **(Fig. 4.8)** was devoid of any tags that could affect the detection of the PS1 variant in subsequent experiments. This optimal condition formed a vital foundation for the effective execution of the study's subsequent experiments, improving the efficacy of study's experimental approach.

3. Isolation of tRNA

In preparing the CFPS system for the synthesis of functional PS1, the isolation of tRNA was an important step. Both the yield and the efficiency of extraction had to be analyzed in order to evaluate the process of isolating tRNA. In the first attempt, the yield of tRNA isolation was 196.491 µg of tRNA **(Fig. 4.9.A)**, indicating the effectiveness of the isolation protocol in producing a sufficient amount of tRNA for the subsequent experiments.

The successful isolation of tRNA was confirmed by gel electrophoresis using Urea-PAGE and agarose gels **(Fig. 4.9. A&B)**. The results were identical, showing a clear band at the expected size of tRNA. This band confirmed the purity of the isolated tRNA and indicated its suitability for assisting the translation machinery in the CFPS system for PS1 synthesis. Since tRNAs are needed for the synthesis of proteins, they facilitate the transfer of amino acids to the ribosome according to the sequence of mRNA codons. The functionality of the CFPS system depends on successful tRNA isolation and the presence of a pure and intact tRNA.

The success of tRNA isolation ensures that the CFPS system has all the elements needed to produce PS1. This enhanced the stability and consistency of the outcomes of the experiments, allowing for more exploration into the synthesis of PS1 protein and its role in AD research.

4. The optimization of plasmid (pET28a-GFP-PS1) yield

The efficiency of the CFPS system for PS1 was directly affected by the amount of plasmid. The plasmid amount impacts the rate of protein production by affecting the concentration of mRNA transcripts. Therefore, determining the ideal plasmid amount was a crucial step to increasing the amount of protein at the maximum point while minimizing resource usage.

According to the protocol for cell-free protein expression reactions in continuous exchange (dialysis) (Biotech, 2014), the plasmid amount should be varied between 0.6 and 1.5 µg in 50 µL tubes. The following amounts were tested to determine the optimal amount of plasmid required for expression: 0, 0.6, 0.8, 1.0, 1.2, and 1.5 µg, respectively. In this part of the study, a fluorescence versus concentration curve was generated to determine the relationship between the amount of pET28a-GFP-PS1 plasmid and the expressed protein concentration **(Fig. 4.10)**. The curve showed a direct relationship, indicating a dose-dependent response; an increase in the amount of pET28a-GFP-PS1 produces a higher concentration of expressed protein **(Fig. 4.10)**. By analyzing this curve, the optimal amount of plasmid would be determined, as it is the amount that gave the maximum concentration of protein when using the lowest amounts of components of translation **(Fig. 4.10)**. The curve showed that the highest concentration of protein was produced when 1.5 µg of the pET28a-GFP-PS1 plasmid was used.

Determining the optimal plasmid amount has implications for the subsequent experiments. A standard parameter for the reactions of protein expression must be provided according to the optimal plasmid amount to ensure a constant and repeatable outcome from the experiments of

study (Jiang et al., 2021; Kim et al., 2020). Moreover, the plasmid optimization step provides a guide for the component amounts, allowing for cost and resource usage reduction.

The optimal plasmid amount condition serves as the foundational aspect for further experiments into the synthesis of PS1 research, offering a reliable platform for investigating the pathogenesis of AD and potential treatment approaches.

5. The Cell-Free Protein synthesis (CFPS) system

The western blot analysis of the CFPS system of PS1 protein gave significant observations. Despite the optimization efforts, all experimental groups showed bands related to the truncated protein **(Fig. 4.11)**. This indicated incomplete synthesis of the protein, premature translation termination, or limitation in the post-transitional modification, such as the lack of essential modification co-factors or enzymes that prevent the generation of full-length protein (Gao et al., 2018; Venkat et al., 2019). These issues prove that the in vitro system works effectively, but the presence of the amber codon can cause significant complications. This contrasts with the findings of Schultz et al. (2001), who effectively developed this system. Schultz showed that the full-length expression of proteins is possible and the specific site incorporation of UAA can be achieved. This contrast could be due to the differences in experimental conditions or the components of the system, which may affect the efficiency of the UAA incorporation at the site of interest.

Limitations:

The truncated protein bands indicated the complexity of the CFPS system to produce PS1 protein **(Fig. 4.11)**. Various factors may cause this, including:

1) Challenges of optimization of the CFPS system

1. Optimization of Reaction conditions:

Unfavorable reaction conditions, a reduction in the energy supply, or a limitation in the translation machinery (Dondapati et al., 2020). Adjusting the parameters of the reaction, like pH, temperature, and the concentration of magnesium, could enhance the ability of the system to synthesize full-length PS1.

2. Optimization of Translation factors and cofactors:

The efficiency of protein expression could be enhanced by modifying the translation machinery, including the supplementation of translation factors and cofactors (Batista et al., 2021), ribosome engineering and recycling (Nürenberg-Goloub & Tampé, 2019), codon optimization, or mRNA modifications (Bae & Coller, 2022).

3. Optimization of Induction time:

Schultz et al.'s research (Young et al., 2010) suggested that induction timing could enhance the efficiency of protein production. This involves optimizing the CFPS system, as the protocol followed was excluded the induction step.

4. Optimization of Concentration of UAA:

The research by Schultz et al. (Young et al., 2010) suggested also optimizing the concentration of the UAA, which is pBpa in this research. And the research of Fu et al. (Fu et al., 2022) proposed developing aaRS\tRNA pairs to establish a reliable framework for many applications of GCE.

2) tRNA isolation challenge:

The promoter of the pETVOL-tRNA vector was the araBAD promoter, and the pET15b-PS1 vector was the T7 promoter, and the T7 polymerase was induced in this system, which means the T7 polymerase will not work to produce tRNA. Because of this, the tRNA was isolated first and then inserted it into this CFPS system. This resulted in two limitations:

1. The isolation process of tRNA:

The isolation process was performed on all tRNAs specific to BL21 Star™ (DE3) cells, along with the target tRNA ($tRNA_{CUA}^{opt}$). The concentration of tRNA that was introduced to this system was related to tRNA, not just the $tRNA_{CUA}^{opt}$. This means that the concentration of $tRNA_{CUA}^{opt}$ was unknown, and perhaps it is too low. As a result, the $tRNA_{CUA}^{opt}$ amount might be insufficient to allow the insertion of UAA into the growing polypeptide.

2. The competition of tRNAs:

Adding all tRNAs could increase the competition of tRNAs for several important factors and components involved in the processes of translation and expression of proteins within this system, including amino acids, ribosomes, the resources of energy, aaRS, and elongation factors. This leads to a reduction in the amount of proteins that were correctly translated, an effect on the overall yield of proteins, a destabilization of the CFPS system, a decline in the accuracy of the translation machinery, and the use of tRNA.

Following the findings of Schultz et al.'s research (Young et al., 2010) to constructe the pETVOL-$tRNA_{CUA}^{opt}$ plasmid with the T7 promoter and then inserting it into the CFPS system may yield the expected results of this system.

3) Competition with release factor 1 (RF1):

one of the most important factors affecting the validity of CFPS systems is the competition between the UAA and the release factor 1 (RF1) at the ribosome during the translation process (Wals & Ovaa, 2014). When RF1 recognizes the amber codon, it terminates the translation. As a result, the truncated protein is produced (Hong et al., 2014). Schultz et al.'s research (Young et al., 2010) demonstrated that the standard lysate-based CFPS system is robust and more efficient for incorporating UAA into proteins. Therefore, obtaining lysate from an RF1-deficient engineered E. coli strain could solve this challenge. These strains are

genetically modified to lack or carry mutations in the RF1 gene (Diago-Navarro et al., 2009). Hong et al.'s research provided a technique to enhance the lysate-based CFPS system by engineering an E. coli strain lacking RF1 (Hong et al., 2014). The development of a gnomically engineered RF1-deficient E. coli strain represents an important milestone in synthetic biology (Martin et al., 2018). Roy et al.'s research (Roy et al., 2020) suggested modulating the levels of RF1 and altering the context of the sequence around the amber codon would improve the incorporation of the UAA process at the interested site.

4) The activity of Bpa-RS:

The activity of Bpa-RS was not tested, which could be one of the causes leading to the failure of the CFPS system. To counter this, utilizing the method of measuring the activity as described by Cestari and Stuart (Cestari & Stuart, 2013) could be advantageous.

Solving those limitations is important to enhance the effectiveness of CFPS systems in a range of applications, including protein engineering, pharmaceutical drug discovery, and therapeutic protein synthesis (Brookwell, Oza, & Caschera, 2021).

The efficiency and fidelity of the production of pBpa-labeled PS1 protein can be enhanced by employing the strategies suggested by Schultz et al. and other relevant research. This progress will greatly advance the goals of this study and offer valuable information to the larger scientific community.

6. Conclusion

CFPS needs carefully designed DNA templates and functional aa-RS capable of incorporating pBpa with its tRNA. Moreover, it requires the addition and optimization of the quantities and concentrations of all components required for the translation process.

This study solved several aspects of the CFPS system of PS1 protein synthesis. Crucial findings include the following: Successful analysis of the plasmids; effective expression and

purification of Bpa-RS; isolation of tRNA; optimization of the plasmid amount; and evaluation of outcomes from the CFPS system for PS1 protein.

Despite the efforts of the optimization of the CFPS system, the incomplete synthesis of full-length PS1 remains a major obstacle of this study. This limitation could be attributed to difficulties in achieving effective transcription and translation processes under the experiment's conditions. The reliability and efficiency of CFPS systems can be enhanced by addressing the recognized limitations and adjusting the experimental parameters.

Since PS1 contributes to the onset of AD, its synthesis is particularly significant. This study contributes to this discipline by emphasizing the potential of the CFPS system for generating complex proteins.

Future research directions

Improving the CFPS system through more optimization steps will be useful to produce full-length proteins labelled with UAA at the targeted site. When the unnatural amino acid pBpa is site-specifically incorporated into recombinant proteins, it will help photocross-linking between the PS1 and other subunit of the GS complex for example Pen2. This, in turn, helps to obtain a deeper understanding of the enzyme’s complex, function, and potential drug targets in the enzyme (Hino et al., 2005) by using MS and other structural techniques (Leitner et al., 2016). Gaining functional and structural insights into GS could facilitate the designing of novel therapies for AD and related conditions.

References

(NEB), N. E. B. (2024). Analysis of Nucleic Acid Concentration and Purity. https://www.neb.com/en//media/nebus/files/applicationnotes/technote_mvs_analysis_of_nucleic_acid_concentration_and_purity.pdf?rev=c24cea043416420d84fb6bf7b554dbbb

2024, S.-A. n. d. (July 5, 2024). Transformation Protocol. https://www.sigmaaldrich.com/DE/en/technical-documents/protocol/genomics/cloning-and-expression/restriction-enzyme-digest-protocol

Abcam. Western Blot Protocol.

https://www.abcam.com/en-us/technical resources/protocols/western-blot

Adachi, J., Katsura, K., Seki, E., Takemoto, C., Shirouzu, M., Terada, T., Mukai, T., Sakamoto, K., & Yokoyama, S. (2019, Jan 24). Cell-Free Protein Synthesis Using S30 Extracts from Escherichia coli RFzero Strains for Efficient Incorporation of Non-Natural Amino Acids into Proteins. Int J Mol Sci, 20(3). https://doi.org/10.3390/ijms20030492

Albright, L. M. S., Barton E. (2024). Denaturing Polyacrylamide Gel Electrophoresis. https://deepblue.lib.umich.edu/bitstream/handle/2027.42/143785/cpnca03b.pdf?sequence=1

Alzheimer's disease facts and figures. (2022, Apr). Alzheimers Dement, 18(2024), 700-789. 2022 https://doi.org/10.1002/alz.12638

Avcilar-Kucukgoze, I., Gamper, H., Hou, Y. M., & Kashina, A. (2020, Dec 18). Purification and Use of tRNA for Enzymatic Post-translational Addition of Amino Acids to Proteins. STAR Protoc, 1(3), 100207. https://doi.org/10.1016/j.xpro.2020.100207

Bae, H., & Coller, J. (2022, Apr 21). Codon optimality-mediated mRNA degradation: Linking translational elongation to mRNA stability. Mol Cell, 82(8), 1467-1476. https://doi.org/10.1016/j.molcel.2022.03.032

Batista, A. C., Soudier, P., Kushwaha, M., & Faulon, J. L. (2021, Mar). Optimising protein synthesis in cell-free systems, a review. Eng Biol, 5(1), 10-19. https://doi.org/10.1049/enb2.12004

Belin, D., & Puigbò, P. (2022, Mar 16). Why Is the UAG (Amber) Stop Codon Almost Absent in Highly Expressed Bacterial Genes? Life (Basel), 12(3). https://doi.org/10.3390/life12030431

Biolabs, N. E. (2012). Transformation Protocol,Bio-Rad. Bulletin_6376.pdf

Biotech, C. (2014). Cell-Free Lysate Normal Protocol. https://cube-biotech.com/media/40/29/dc/1668091046/Cell-Free%20Lysate%20Normal%20Protocoll.pdf

Boulder, U. o. C. (2018). EmulsiFlex-C3 Homogenizer Protocol. https://colorado.edu/lab/biochem-instruments/sites/default/files/attached files/emulsiflex_c3_homogenizer_protocol_2018_0.pdf

Breijyeh, Z., & Karaman, R. (2020, Dec 8). Comprehensive Review on Alzheimer's Disease: Causes and Treatment. Molecules, 25(2024). https://doi.org/10.3390/molecules25245789

Castro, T. G., Melle-Franco, M., Sousa, C. E. A., Cavaco-Paulo, A., & Marcos, J. C. (2023, Jun 12). Non-Canonical Amino Acids as Building Blocks for Peptidomimetics: Structure, Function, and Applications. Biomolecules, 13(6). https://doi.org/10.3390/biom13060981

Cestari, I., & Stuart, K. (2013, Apr). A spectrophotometric assay for quantitative measurement of aminoacyl-tRNA synthetase activity. J Biomol Screen, 18(2024), 490-497. https://doi.org/10.1177/1087057112465980

Chow, V. W., Mattson, M. P., Wong, P. C., & Gleichmann, M. (2010, Mar). An overview of APP processing enzymes and products. Neuromolecular Med, 12(1), 1-12. https://doi.org/10.1007/s12017-009-8104-z

Cui, Z., Johnston, W. A., & Alexandrov, K. (2020). Cell-Free Approach for Non-canonical Amino Acids Incorporation Into Polypeptides. Front Bioeng Biotechnol, 8, 1031. https://doi.org/10.3389/fbioe.2020.01031

Dey, S., Pal, A., Chakrabarti, P., & Janin, J. (2010, Apr 23). The subunit interfaces of weakly associated homodimeric proteins. J Mol Biol, 398(1), 146-160. https://doi.org/10.1016/j.jmb.2010.02.020

Diago-Navarro, E., Mora, L., Buckingham, R. H., Díaz-Orejas, R., & Lemonnier, M. (2009, Jan). Novel Escherichia coli RF1 mutants with decreased translation termination activity and increased sensitivity to the cytotoxic effect of the bacterial toxins Kid and RelE. Mol Microbiol, 71(1), 66-78. https://doi.org/10.1111/j.1365-2958.2008.06510.x

Dondapati, S. K., Stech, M., Zemella, A., & Kubick, S. (2020, Jun). Cell-Free Protein Synthesis: A Promising Option for Future Drug Development. BioDrugs, 34(3), 327-348. https://doi.org/10.1007/s40259-020-00417-y

Forné, I., Ludwigsen, J., Imhof, A., Becker, P. B., & Mueller-Planitz, F. (2012, Apr). Probing the conformation of the ISWI ATPase domain with genetically encoded photoreactive crosslinkers and mass spectrometry. Mol Cell Proteomics, 11(2024), M111.012088. https://doi.org/10.1074/mcp.M111.012088

Fraering, P. C. (2007, Dec). Structural and Functional Determinants of gamma-Secretase, an Intramembrane Protease Implicated in Alzheimer's Disease. Curr Genomics, 8(8), 531-549. https://doi.org/10.2174/138920207783769521

Fu, X., Huang, Y., & Shen, Y. (2022). Improving the Efficiency and Orthogonality of Genetic Code Expansion. Biodes Res, 2022, 9896125. https://doi.org/10.34133/2022/9896125

Gao, W., Bu, N., & Lu, Y. (2018, Sep 25). [Recent advances in cell-free unnatural protein synthesis]. Sheng Wu Gong Cheng Xue Bao, 34(9), 1371-1385. https://doi.org/10.13345/j.cjb.180203

G-Biosciences. Coomassie blue staining G250 protocol. https://cdn.gbiosciences.com/pdfs/protocol/786-497_protocol.pdf

Goel, P., Chakrabarti, S., Goel, K., Bhutani, K., Chopra, T., & Bali, S. (2022). Neuronal cell death mechanisms in Alzheimer's disease: An insight. Front Mol Neurosci, 15, 937133. https://doi.org/10.3389/fnmol.2022.937133

Gregorio, N. E., Levine, M. Z., & Oza, J. P. (2019, Mar 12). A User's Guide to Cell-Free Protein Synthesis. Methods Protoc, 2(1). https://doi.org/10.3390/mps2010024

Gulisano, W., Maugeri, D., Baltrons, M. A., Fà, M., Amato, A., Palmeri, A., D'Adamio, L., Grassi, C., Devanand, D. P., Honig, L. S., Puzzo, D., & Arancio, O. (2018). Role of Amyloid-β and Tau Proteins in Alzheimer's Disease: Confuting the Amyloid Cascade. J Alzheimers Dis, 64(s1), S611-s631. https://doi.org/10.3233/jad-179935

Guo, Q. R., & Cao, Y. J. (2024, May 7). Applications of genetic code expansion technology in eukaryotes. Protein Cell, 15(5), 331-363. https://doi.org/10.1093/procel/pwad051

Hampel, H., Hardy, J., Blennow, K., Chen, C., Perry, G., Kim, S. H., Villemagne, V. L., Aisen, P., Vendruscolo, M., & Iwatsubo, T. (2021). The amyloid-β pathway in Alzheimer's disease. Molecular psychiatry, 26(10), 5481-5503.

Hino, N., Okazaki, Y., Kobayashi, T., Hayashi, A., Sakamoto, K., & Yokoyama, S. (2005, Mar). Protein photo-cross-linking in mammalian cells by site-specific incorporation of a photoreactive amino acid. Nat Methods, 2(3), 201-206. https://doi.org/10.1038/nmeth739

Hoenger Ramazanova, R. D., Roumeliotis, T. I., Wright, J. C., & Choudhary, J. S. (2024, Nov 1). PhoXplex: Combining Phospho-enrichable Cross-Linking with Isobaric Labeling for Quantitative Proteome-Wide Mapping of Protein Interfaces. J Proteome Res, 23(11), 5209-5220. https://doi.org/10.1021/acs.jproteome.4c00567

Hong, S. H., Ntai, I., Haimovich, A. D., Kelleher, N. L., Isaacs, F. J., & Jewett, M. C. (2014, Jun 20). Cell-free protein synthesis from a release factor 1 deficient Escherichia coli activates efficient and multiple site-specific nonstandard amino acid incorporation. ACS Synth Biol, 3(6), 398-409. https://doi.org/10.1021/sb400140t

https://www.bio-rad.com/webroot/web/pdf/lsr/literature/Bulletin_6376.pdf

https://www.neb.com/en/protocols/2012/05/21/transformation-protocol

https://www.sigmaaldrich.com/DE/en/technical-documents/protocol/genomics/cloning-and-expression/restriction-enzyme-digest-protocol

Hur, J. Y. (2022, Apr). γ-Secretase in Alzheimer's disease. Exp Mol Med, 54(2024), 433-446. https://doi.org/10.1038/s12276-022-00754-8

in its Native Context

Information, N. C. f. B. (2024). https://pubchem.ncbi.nlm.nih.gov/compound/4-Benzoyl-l-phenylalanine.

Jiang, N., Ding, X., & Lu, Y. (2021, Jan 15). Development of a robust Escherichia coli-based cell-free protein synthesis application platform. Biochem Eng J, 165, 107830. https://doi.org/10.1016/j.bej.2020.107830

Jordà-Siquier, T., Petrel, M., Kouskoff, V., Smailovic, U., Cordelières, F., Frykman, S., Müller, U., Mulle, C., & Barthet, G. (2022, Nov). APP accumulates with presynaptic proteins around amyloid plaques: A role for presynaptic mechanisms in Alzheimer's disease? Alzheimers Dement, 18(11), 2099-2116. https://doi.org/10.1002/alz.12546

Kauer, J. C., Erickson-Viitanen, S., Wolfe, H. R., Jr., & DeGrado, W. F. (1986, Aug 15). p-Benzoyl-L-phenylalanine, a new photoreactive amino acid. Photolabeling of calmodulin with a synthetic calmodulin-binding peptide. J Biol Chem, 261(23), 10695-10700.

Kedia, S., Mandal, K., Netrakanti, P. R., Jose, M., Sisodia, S. S., & Nair, D. (2021, Oct 13). Nanoscale organization of Nicastrin, the substrate receptor of the γ-secretase complex, as independent molecular domains. Mol Brain, 14(1), 158. https://doi.org/10.1186/s13041-021-00855-x

Khambhati, K., Bhattacharjee, G., Gohil, N., Braddick, D., Kulkarni, V., & Singh, V. (2019). Exploring the Potential of Cell-Free Protein Synthesis for Extending the Abilities of Biological Systems. Front Bioeng Biotechnol, 7, 248. https://doi.org/10.3389/fbioe.2019.00248

Kim, J., Copeland, C. E., Seki, K., Vögeli, B., & Kwon, Y. C. (2020). Tuning the Cell-Free Protein Synthesis System for Biomanufacturing of Monomeric Human Filaggrin. Front Bioeng Biotechnol, 8, 590341. https://doi.org/10.3389/fbioe.2020.590341

Kim, Y., Cho, S., Kim, J. C., & Park, H. S. (2024). tRNA engineering strategies for genetic code expansion. Front Genet, 15, 1373250. https://doi.org/10.3389/fgene.2024.1373250

Kolarova, M., García-Sierra, F., Bartos, A., Ricny, J., & Ripova, D. (2012). Structure and pathology of tau protein in Alzheimer disease. Int J Alzheimers Dis, 2012, 731526. https://doi.org/10.1155/2012/731526

Lee, D., Kim, J. G., Kim, T. W., & Choi, J. I. (2024, May 24). Development of orthogonal aminoacyl-tRNA synthetase mutant for incorporating a non-canonical amino acid. AMB Express, 14(1), 60. https://doi.org/10.1186/s13568-024-01706-3

Lee, K. J., Kang, D., & Park, H. S. (2019, May 31). Site-Specific Labeling of Proteins Using Unnatural Amino Acids. Mol Cells, 42(5), 386-396. https://doi.org/10.14348/molcells.2019.0078

Lee, P. Y., Costumbrado, J., Hsu, C. Y., & Kim, Y. H. (2012, Apr 20). Agarose gel electrophoresis for the separation of DNA fragments. J Vis Exp(62). https://doi.org/10.3791/3923

Leitner, A., Faini, M., Stengel, F., & Aebersold, R. (2016, Jan). Crosslinking and Mass Spectrometry: An Integrated Technology to Understand the Structure and Function of Molecular Machines. Trends Biochem Sci, 41(1), 20-32. https://doi.org/10.1016/j.tibs.2015.10.008

Li, Y., Bohm, C., Dodd, R., Chen, F., Qamar, S., Schmitt-Ulms, G., Fraser, P. E., & St George-Hyslop, P. H. (2014, Dec 18). Structural biology of presenilin 1 complexes. Mol Neurodegener, 9, 59. https://doi.org/10.1186/1750-1326-9-59

Livingston, G., Huntley, J., Sommerlad, A., Ames, D., Ballard, C., Banerjee, S., Brayne, C., Burns, A., Cohen-Mansfield, J., & Cooper, C. (2020). Dementia prevention, intervention, and care: 2020 report of the Lancet Commission. The Lancet, 396(10248), 413-446.

Luo, J. E., & Li, Y. M. (2022, Jan 4). Turning the tide on Alzheimer's disease: modulation of γ-secretase. Cell Biosci, 12(1), 2. https://doi.org/10.1186/s13578-021-00738-7

Maharjan, A., & Park, J. H. (2023, Dec). Cell-free protein synthesis system: A new frontier for sustainable biotechnology-based products. Biotechnol Appl Biochem, 70(6), 2136-2149. https://doi.org/10.1002/bab.2514

Mahmood, T., & Yang, P. C. (2012, Sep). Western blot: technique, theory, and trouble shooting. N Am J Med Sci, 4(9), 429-434. https://doi.org/10.4103/1947-2714.100998

Majekodunmi, T., Britton, D., & Montclare, J. K. (2024, Aug 14). Engineered Proteins and Materials Utilizing Residue-Specific Noncanonical Amino Acid Incorporation. Chem Rev, 124(15), 9113-9135. https://doi.org/10.1021/acs.chemrev.3c00855

Martin, R. W., Des Soye, B. J., Kwon, Y. C., Kay, J., Davis, R. G., Thomas, P. M., Majewska, N. I., Chen, C. X., Marcum, R. D., Weiss, M. G., Stoddart, A. E., Amiram, M., Ranji Charna, A. K., Patel, J. R., Isaacs, F. J., Kelleher, N. L., Hong, S. H., & Jewett, M. C. (2018, Mar 23). Cell-free protein synthesis from genomically recoded bacteria enables multisite incorporation of noncanonical amino acids. Nat Commun, 9(1), 1203. https://doi.org/10.1038/s41467-018-03469-5

Medeiros, R., Baglietto-Vargas, D., & LaFerla, F. M. (2011, Oct). The role of tau in Alzheimer's disease and related disorders. CNS Neurosci Ther, 17(5), 514-524. https://doi.org/10.1111/j.1755-5949.2010.00177.x

Melnikov, S. V., & Söll, D. (2019, Apr 19). Aminoacyl-tRNA Synthetases and tRNAs for an Expanded Genetic Code: What Makes them Orthogonal? Int J Mol Sci, 20(8). https://doi.org/10.3390/ijms20081929

Miyazaki, R., Akiyama, Y., & Mori, H. (2020, Feb). A photo-cross-linking approach to monitor protein dynamics in living cells. Biochim Biophys Acta Gen Subj, 1864(2024), 129317. https://doi.org/10.1016/j.bbagen.2019.03.003

Morris, R., Black, K. A., & Stollar, E. J. (2022, Aug 10). Uncovering protein function: from classification to complexes. Essays Biochem, 66(3), 255-285. https://doi.org/10.1042/ebc20200108

Murphy, M. P., & LeVine, H., 3rd. (2010). Alzheimer's disease and the amyloid-beta peptide. J Alzheimers Dis, 19(1), 311-323. https://doi.org/10.3233/jad-2010-1221

Nasb, M., Tao, W., & Chen, N. (2024, Feb 1). Alzheimer's Disease Puzzle: Delving into Pathogenesis Hypotheses. Aging Dis, 15(1), 43-73. https://doi.org/10.14336/ad.2023.0608

Nie, P., Vartak, A., & Li, Y. M. (2020, Sep). γ-Secretase inhibitors and modulators: Mechanistic insights into the function and regulation of γ-Secretase. Semin Cell Dev Biol, 105, 43-53. https://doi.org/10.1016/j.semcdb.2020.03.002

Nikić-Spiegel, I. (2020, Nov 16). Expanding the Genetic Code for Neuronal Studies. Chembiochem, 21(22), 3169-3179. https://doi.org/10.1002/cbic.202000300

Nordvall, G., Lundkvist, J., & Sandin, J. (2023). Gamma-secretase modulators: a promising route for the treatment of Alzheimer's disease. Front Mol Neurosci, 16, 1279740. https://doi.org/10.3389/fnmol.2023.1279740

Nürenberg-Goloub, E., & Tampé, R. (2019, Dec 18). Ribosome recycling in mRNA translation, quality control, and homeostasis. Biol Chem, 401(1), 47-61. https://doi.org/10.1515/hsz-2019-0279

O'Brien, R. J., & Wong, P. C. (2011). Amyloid precursor protein processing and Alzheimer's disease. Annu Rev Neurosci, 34, 185-204. https://doi.org/10.1146/annurev-neuro-061010-113613

Olsauskas-Kuprys, R., Zlobin, A., & Osipo, C. (2013). Gamma secretase inhibitors of Notch signaling. Onco Targets Ther, 6, 943-955. https://doi.org/10.2147/ott.S33766

Ozawa, K., & Loh, C. T. (2014). Site-Specific Incorporation of Unnatural Amino Acids into Proteins by Cell-Free Protein Synthesis. In K. Alexandrov & W. A. Johnston (Eds.), Cell-Free Protein Synthesis: Methods and Protocols (pp. 189-203). Humana Press. https://doi.org/10.1007/978-1-62703-782-2_12

Ozawa, K., & Loh, C. T. (2014). Site-specific incorporation of unnatural amino acids into proteins by cell-free protein synthesis. Methods Mol Biol, 1118, 189-203. https://doi.org/10.1007/978-1-62703-782-2_12

Panza, F., Frisardi, V., Imbimbo, B. P., Capurso, C., Logroscino, G., Sancarlo, D., Seripa, D., Vendemiale, G., Pilotto, A., & Solfrizzi, V. (2010, Oct). REVIEW: γ-Secretase inhibitors for the treatment of Alzheimer's disease: The current state. CNS Neurosci Ther, 16(5), 272-284. https://doi.org/10.1111/j.1755-5949.2010.00164.x

Passeri, E., Elkhoury, K., Morsink, M., Broersen, K., Linder, M., Tamayol, A., Malaplate, C., Yen, F. T., & Arab-Tehrany, E. (2022, Nov 12). Alzheimer's Disease: Treatment Strategies and Their Limitations. Int J Mol Sci, 23(22). https://doi.org/10.3390/ijms232213954

Patel, R. S., Pannala, N. M., & Das, C. (2024, Jun 3). Reading and Writing the Ubiquitin Code Using Genetic Code Expansion. Chembiochem, 25(11), e202400190. https://doi.org/10.1002/cbic.202400190

Peeler, J. C., & Mehl, R. A. (2012). Site-specific incorporation of unnatural amino acids as probes for protein conformational changes. Methods Mol Biol, 794, 125-134. https://doi.org/10.1007/978-1-61779-331-8_8

Petrotchenko, E. V., & Borchers, C. H. (2022, Apr 27). Protein Chemistry Combined with Mass Spectrometry for Protein Structure Determination. Chem Rev, 122(8), 7488-7499. https://doi.org/10.1021/acs.chemrev.1c00302

Pires, M., & Rego, A. C. (2023, Jan 1). Apoe4 and Alzheimer's Disease Pathogenesis-Mitochondrial Deregulation and Targeted Therapeutic Strategies. Int J Mol Sci, 24(1). https://doi.org/10.3390/ijms24010778

Porter, J. J., Heil, C. S., & Lueck, J. D. (2021, Jul). Therapeutic promise of engineered nonsense suppressor tRNAs. Wiley Interdiscip Rev RNA, 12(2024), e1641. https://doi.org/10.1002/wrna.1641

Protocols.io. (2024). Ethanol Precipitation of Nucleic Acids (Eppendorf Tube Method). https://www.protocols.io/view/Ethanol-precipitation-of-nucleic-acids-Eppendorf-t-zewov1qygr24/v1

Rajmohan, R., & Reddy, P. H. (2017). Amyloid-Beta and Phosphorylated Tau Accumulations Cause Abnormalities at Synapses of Alzheimer's disease Neurons. J Alzheimers Dis, 57(2024), 975-999. https://doi.org/10.3233/jad-160612

Roda, A. R., Serra-Mir, G., Montoliu-Gaya, L., Tiessler, L., & Villegas, S. (2022, Aug). Amyloid-beta peptide and tau protein crosstalk in Alzheimer's disease. Neural Regen Res, 17(8), 1666-1674. https://doi.org/10.4103/1673-5374.332127

Roos, C., Kai, L., Haberstock, S., Proverbio, D., Ghoshdastider, U., Ma, Y., Filipek, S., Wang, X., Dötsch, V., & Bernhard, F. (2014). High-level cell-free production of membrane proteins with nanodiscs. Methods Mol Biol, 1118, 109-130. https://doi.org/10.1007/978-1-62703-782-2_7

Roy, G., Reier, J., Garcia, A., Martin, T., Rice, M., Wang, J., Prophet, M., Christie, R., Dall'Acqua, W., Ahuja, S., Bowen, M. A., & Marelli, M. (2020, Jan-Dec). Development of a high yielding expression platform for the introduction of non-natural amino acids in protein sequences. MAbs, 12(1), 1684749. https://doi.org/10.1080/19420862.2019.1684749

Ryman, D. C., Acosta-Baena, N., Aisen, P. S., Bird, T., Danek, A., Fox, N. C., Goate, A., Frommelt, P., Ghetti, B., & Langbaum, J. B. (2014). Symptom onset in autosomal dominant Alzheimer disease: a systematic review and meta-analysis. Neurology, 83(3), 253-260.

Sadigh-Eteghad, S., Sabermarouf, B., Majdi, A., Talebi, M., Farhoudi, M., & Mahmoudi, J. (2015). Amyloid-beta: a crucial factor in Alzheimer's disease. Med Princ Pract, 24(1), 1-10. https://doi.org/10.1159/000369101

Scheltens, P., De Strooper, B., Kivipelto, M., Holstege, H., Chételat, G., Teunissen, C. E., Cummings, J., & van der Flier, W. M. (2021, Apr 24). Alzheimer's disease. Lancet, 397(10284), 1577-1590. https://doi.org/10.1016/s0140-6736(2024)32205-4

Scientific, T. F. (2024). GeneJET Plasmid Maxiprep Protocol. https://www.thermofisher.com/document-connect/document-connect.html?url=https://assets.thermofisher.com/TFS-Assets%2FLSG%2Fmanuals%2FMAN0012654_GeneJET_Plasmid_Maxiprep_UG.pdf

Scientific, T. F. (2024). Nucleic Acid Electrophoresis Workflow. https://www.thermofisher.com/ps/en/home/life-science/cloning/cloning-learning-center/invitrogen-school-of-molecular-biology/na-electrophoresis-education/na-electrophoresis-workflow.html

Sigma-Aldrich. (2024). Restriction Enzyme Digest Protocol

Smith, E., & Collins, I. (2015). Photoaffinity labeling in target- and binding-site identification. Future Med Chem, 7(2024), 159-183. https://doi.org/10.4155/fmc.14.152

Smolskaya, S., Logashina, Y. A., & Andreev, Y. A. (2020, Jan 31). Escherichia coli Extract-Based Cell-Free Expression System as an Alternative for Difficult-to-Obtain Protein Biosynthesis. Int J Mol Sci, 21(3). https://doi.org/10.3390/ijms21030928

Tarasoff-Conway, J. M., Carare, R. O., Osorio, R. S., Glodzik, L., Butler, T., Fieremans, E., Axel, L., Rusinek, H., Nicholson, C., Zlokovic, B. V., Frangione, B., Blennow, K., Ménard, J., Zetterberg, H., Wisniewski, T., & de Leon, M. J. (2015, Aug). Clearance systems in the

brain-implications for Alzheimer disease. Nat Rev Neurol, 11(8), 457-470. https://doi.org/10.1038/nrneurol.2015.119

Tarawneh, R., & Holtzman, D. M. (2012, May). The clinical problem of symptomatic Alzheimer disease and mild cognitive impairment. Cold Spring Harb Perspect Med, 2(5), a006148. https://doi.org/10.1101/cshperspect.a006148

Umanah, G., Huang, L.-Y., Schultz, P. G., Naider, F., & Becker, J. M. . (2009). Incorporation of the Unnatural Amino Acid p-benzoylL-phenylalanine (Bpa) into a G Protein-coupled Receptor

University, S. I. (2024). Coomassie Staining Protocol. https://mass-spec.siu.edu/_common/documents/coomassie-staining-protocol.pdf

Urban, A. S., Pavlov, K. V., Kamynina, A. V., Okhrimenko, I. S., Arseniev, A. S., & Bocharov, E. V. (2021, May 13). Structural Studies Providing Insights into Production and Conformational Behavior of Amyloid-β Peptide Associated with Alzheimer's Disease Development. Molecules, 26(10). https://doi.org/10.3390/molecules26102897

Vadukul, D. M., Gbajumo, O., Marshall, K. E., & Serpell, L. C. (2017, Mar). Amyloidogenicity and toxicity of the reverse and scrambled variants of amyloid-β 1-42. FEBS Lett, 591(5), 822-830. https://doi.org/10.1002/1873-3468.12590

van Tetering, G., & Vooijs, M. (2011, Jun). Proteolytic cleavage of Notch: "HIT and RUN". Curr Mol Med, 11(2024), 255-269. https://doi.org/10.2174/156652411795677972

Venkat, S., Chen, H., Gan, Q., & Fan, C. (2019). The Application of Cell-Free Protein Synthesis in Genetic Code Expansion for Post-translational Modifications. Front Pharmacol, 10, 248. https://doi.org/10.3389/fphar.2019.00248

Wals, K., & Ovaa, H. (2014). Unnatural amino acid incorporation in E. coli: current and future applications in the design of therapeutic proteins. Front Chem, 2, 15. https://doi.org/10.3389/fchem.2014.00015

Wang, X., Zhou, X., Li, G., Zhang, Y., Wu, Y., & Song, W. (2017). Modifications and Trafficking of APP in the Pathogenesis of Alzheimer's Disease. Front Mol Neurosci, 10, 294. https://doi.org/10.3389/fnmol.2017.00294

Yang, G., Miton, C. M., & Tokuriki, N. (2020, Aug). A mechanistic view of enzyme evolution. Protein Sci, 29(8), 1724-1747. https://doi.org/10.1002/pro.3901

Young, T. S., & Schultz, P. G. (2010, Apr 9). Beyond the canonical 20 amino acids: expanding the genetic lexicon. J Biol Chem, 285(15), 11039-11044. https://doi.org/10.1074/jbc.R109.091306

Young, T. S., Ahmad, I., Yin, J. A., & Schultz, P. G. (2010, Jan 15). An enhanced system for unnatural amino acid mutagenesis in E. coli. J Mol Biol, 395(2024), 361-374. https://doi.org/10.1016/j.jmb.2009.10.030

Zhang, H., Wei, W., Zhao, M., Ma, L., Jiang, X., Pei, H., Cao, Y., & Li, H. (2021). Interaction between Aβ and Tau in the Pathogenesis of Alzheimer's Disease. Int J Biol Sci, 17(9), 2181-2192. https://doi.org/10.7150/ijbs.57078

Zhang, L., Lin, X., Wang, T., Guo, W., & Lu, Y. (2021). Development and comparison of cell-free protein synthesis systems derived from typical bacterial chassis. Bioresour Bioprocess, 8(1), 58. https://doi.org/10.1186/s40643-021-00413-2

Zhang, X., Li, Y., Xu, H., & Zhang, Y. W. (2014). The γ-secretase complex: from structure to function. Front Cell Neurosci, 8, 427. https://doi.org/10.3389/fncel.2014.00427

Zhang, Y., Chen, H., Li, R., Sterling, K., & Song, W. (2023, Jun 30). Amyloid β-based therapy for Alzheimer's disease: challenges, successes and future. Signal Transduct Target Ther, 8(1), 248. https://doi.org/10.1038/s41392-023-01484-7

Zhao, S., & Liu, D. (2023). Applications of genetic code expansion and photosensitive UAAs in studying membrane proteins. Open Life Sci, 18(1), 20220752. https://doi.org/10.1515/biol-2022-0752

Zhou, Y., Sun, Y., Ma, Q. H., & Liu, Y. (2018, Jun 29). Alzheimer's disease: amyloid-based pathogenesis and potential therapies. Cell Stress, 2(7), 150-161. https://doi.org/10.15698/cst2018.07.143

Zhou, Z. D., Chan, C. H., Ma, Q. H., Xu, X. H., Xiao, Z. C., & Tan, E. K. (2011, Jul-Aug). The roles of amyloid precursor protein (APP) in neurogenesis: Implications to pathogenesis and therapy of Alzheimer disease. Cell Adh Migr, 5(2024), 280-292. https://doi.org/10.4161/cam.5.4.16986

ادخال حمض أميني غير طبيعي يسمى (بينزويل ل فينيل الانين) في الوحدة البنائية (بريسنيلين 1) من انزيم غاما سيكراتاز خارج الخلية

اسم الطالب: هبه شوكت عارف كميل

أ.د. هلال زيد

أ.د. جورج لبان

د. صبا إسماعيل

د. رمزي شواهنه

ملخص

يعتبر الزهايمر من الامراض العصبية التي تشكل تحديا كبيرا للعلماء في هذا العصر والدراسات نحو فهم الاسباب المؤدية لحدوثه بازدياد مع ازدياد اعداد المصابين به. هذا المرض ما زال دواء لغاية الان مع انه تم اكتشافه قبل ما يقارب القرن, الامر الذي يستدعي تسليط الضوء عليه ويزيد من اهمية التركيز على دراسة اسباب حدوثه وضرورة فهم الياته الجزيئية. الانزيم (γ–secretase) وخاصة الوحدة البنائية منه PS1 لها دور كبير في تراكم اللويحات الأميلويدية وتكوينها, التي يعتقد ان تراكمها سبب من مسببات مرض الزهايمر, حيث تم ملاحظة تراكم نسبة عالية من هذه اللويحات افي ادمغة المصابين بهذا المرض.

تهدف هذه الدراسة الى تصميم نظام لإنتاج الوحدة البنائية PS1دون استخدام خلايا واستخدام استراتيجية اضافة حمض اميني غير طبيعي ((p–Benzoyl–L–phenylalanine (pBpa) الى موقع 190من تسلسل الاحماض الامينية للبروتين PS1, حيث ان نجحت اضافة هذا الحمض الاميني للبروتين انه سيصبح قادراً على ربط الوحدة البنائية PS1مع وحدة بنائية مجاورة لها عند تعريضه لموجات UV وباستخدام تقنية MS سيتم التعرف على الية ارتباط هذه الوحدات ببعض بالفراغ وسيتم معرفة ابعادهم الثلاثية. ولتصميم هذا النظام الغير حيوي يتطلب تصميم بلازميدات معينة بتعديلات مطلوبة لمحاولة انتاج بروتين حامل حمض اميني غير طبيعي وايضا يلزمه استخلاص tRNA وBpa–RS بطرق مناسبة ومن ثم اضافتهم الى هذا النظام ومعايرة هذا النظام من حيث كمية البلازميدات المطلوب اضافتها للنظام. يتبعها تطبيق هذا النظام وتحليل النتائج باستخدام تقنيات western blot, Coomassie Blue Staining and Gel electrophoresis technique.

بالرغم من النجاح في استخلاص كلا tRNA وBpa-RS، الا ان بعد تطبيق النظام الغير حيوي بإضافة كلا من هاتين المادتين واضافة البلازميد المطلوب وكل مكونات النسخ والترجمة وانتاج البروتين المستخلصة من البكتريا. النظام سيسهم في انتاج PS1 غير الكامل وحجم البروتين اقل من الطبيعي.

بالرغم من ان هدف التجربة هو انتاج PS1 كامل وفعال لم يتحقق، الا ان التجربة سلطت الضوء على التحديات التي تواجه انتاج البروتينات المعقدة مثل PS1. بعد هذه الدراسة يستلزم دراسات اخرى تركز على معايرة النظام وتتبع المشكلة التي قد تكون حدثت في أحد مراحل النسخ والترجمة في سبيل انتاج بروتين كامل فعال، ان تتبع المشكلة والفهم العميق للنظام سيساعد في الوصول للهدف الرئيسي للتجربة، وسيبنى عليه دراسات اخرى في سبيل فهم الشكل الثلاثي لإنزيم γ-secretase. قد تسهم هذه الدراسة في شق الطريق للإنتاج دواء وعلاجات لمرض هو الان معضلة كبيرة للعلماء الا وهو الزهايمر.

الكلمات المفتاحية: مرض الزهايمر, انزيم, علاج.